

US EPA ARCHIVE DOCUMENT



April 4, 2011

154.002.009.001

Mr. Daniel Siegfried, Managing Attorney  
Alliant Energy Corporate Services  
Legal Department  
200 First Street SE  
PO Box 351  
Cedar Rapids, IA 52406-0351

Re: Response to Additional Activities Request  
United States Environmental Protection Agency  
March 29, 2011 Response to Alliant's March 23, 2011 Submittal

Dear Mr. Siegfried;

Aether DBS, LLC is responding to additional activities requests A, B and F from the United States Environmental Protection Agencies (USEPA's) letter to Alliant Energy Corporation (Alliant) of March 29, 2011. For completion in our response, the USEPA request is repeated along with Aether's response.

- A. *Conduct a formal dam break analysis based on a catastrophic failure of the Economizer Ash Pond, with accompanying calculations and reference material, signed by a Professional Engineer on letterhead.*

The calculations and references in support of the dam break analysis summarized in Alliant's March 23, 2011 submittal are enclosed as Attachment A. The analysis is based on the momentum principals of Saint-Venant. The liquefied ash is conservatively treated as water with no viscosity. The force of the released wave on the clay embankment at the north end of the Upper Ash Pond is based on the conservation of energy.

The release of a negative roll wave as presented in Chow, is based on an infinite source of water (liquefied soil). The equation projects that the flow reaches a constant thickness forever. The Economizer Ash Pond is not infinite and the spreading of liquefaction in the Economizer Ash Pond will run out of source at about the same time it reaches the Upper Ash Pond north embankment. In support of this finite limiting concept, the TVA Kingston ash pile ran out of source before the entire pond contents flowed out of the pond area.

## CONFIDENTIAL BUSINESS INFORMATION

When the flowing ash stops it stops suddenly and reverts to a solid form. From experience at Kingston the change from fluid behavior to solid behavior occurs at a unit weight of 70 to 75 pounds per cubic foot. For conservatism, Aether assumed that the unit weight of the flowing ash was 95 pounds per cubic foot when it contacts the Upper Ash Pond embankment. The resultant pressure will not move the clay embankment.

Aether trusts that a review of the calculations and references in conjunction with the Figures showing the true scale variations of site features will assure the USEPA that the contents of a liquefied Economizer Ash Pond will remain within the confines of the Economizer Ash Pond and the Upper Ash Pond at the Burlington Generating Station.

The work by Aether was performed by or under the supervision of Mr. Timothy J. Harrington, P.E. who has over 35-years of engineering experience including significant work on the liquefaction of soils and the effects of earthquakes on structures founded on soil. Mr. Harrington directed work at TVA Kingston to remove ash from the Emory River and is experienced with the ways that ash handles when in a liquefied state. Mr. Harrington is a registered professional engineer in ten states and is responsible for the technical content of Aether's presentation.

*B. Conduct a hydraulic study that verifies only water is released in the event of an Economizer embankment failure.*

If static liquefaction results in fluidized economizer ash flowing north into the Upper Ash Pond the flowing ash would displace water and settled fluid ash in the Upper Ash Pond. The displaced water would flow to the western end of the Upper Ash Pond and up and over the crest of the Upper Ash Pond. The liquefied mass of Economizer Ash would be arrested at the Upper Ash Embankment with all motion complete in less than 10-minutes (Attachment A).

Aether estimates that the Upper Ash Pond contains approximately 1,000,000 cubic feet of water and that 50% of the water will flow to the western end of the pond and 50% will go over the top of the Upper Ash Pond embankment and enter the Lower Ash Pond, Attachment B. The rate of flow over the top of the embankment will be proportional to the arrival of the liquefied Economizer Ash with 90% of the flow in the first three minutes and the remaining 10% over the next seven minutes.

The water overtopping the Upper Ash Pond will be detained in the Lower Ash Pond and will result in an increase of the Lower Ash Pond water elevation by approximately 8-inches. The flow over the Lower Ash Pond discharge weir will increase by three times the normal flow and the first 25% of the surge of water will take approximately 2.5 hours to discharge from the Lower Ash Pond. Half of the displaced water will take about 6 hours to discharge and approximately 24 hours to drain approximately 90% of the displaced water over the lower ash pond weir structure. The retention will provide more than adequate time for the fluid ash from the Upper Ash Pond to settle prior to discharge of the water to the Mississippi River.

## CONFIDENTIAL BUSINESS INFORMATION

- F. *Install slope inclinometers in association with the new borings. The slope inclinometer data should provide locations and magnitude of horizontal movement within the Economizer Ash Pond embankment and underlying materials. Periodic measurements should provide data on the rate of movement. This data should be part of a geotechnical report that describes the actions taken by Alliant to address the embankment stability issue.*

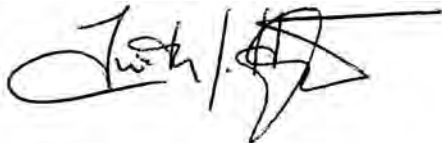
Aether does not understand how the use of slope inclinometers would lower the ash release risk at the Burlington Station. The failure mechanisms that would lead to liquefaction flow are either a design level earthquake or a static shear event that causes static liquefaction of the Economizer Ash Pond. Both of these events would be sudden without movement of the embankments prior to the liquefaction event. The slope inclinometers would not show movement prior to the event.

Liquefaction is triggered by sudden increases of pore water pressure in fine sands, silts or sensitive clays. Sudden means occurring in less than a minute. These increases may result from the cyclic shearing that occurs in the strong motion of a large earthquake or by the sudden shearing failure of a slope that is saturated. In both cases the slope will not be moving prior to the shearing event. At TVA Kingston the slope failed due to increased seepage pressure and weight from suddenly increasing the hydraulic flow to the pile.

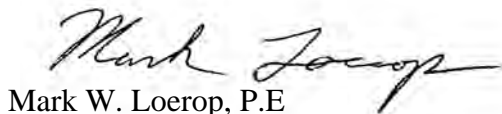
Aether understands that the hydraulic flow to the Economizer Ash Pond has not increased and that Alliant is removing Economizer Ash as it accumulates and taking it off the top of the Economizer Ash Pond.

Aether suggests that we first determine if a clay embankment is present in the eastern half of the north Economizer Ash Pond embankment before making decisions on the use of inclinometers as a monitoring tool. The purpose in that case would be to monitor the relative movements between the embankment and the underlying soil that might be occurring because of increased loadings.

Respectfully,



Timothy J. Harrington, P.E.



Mark W. Loerop, P.E

**Attachment A**  
**Liquefaction Flow Analysis**  
**Economizer Ash Pond**  
**Burlington Generating Station**



SHEET NO. 1 OF 4

PROJECT NO. 154.002.009

DATE 3-22-11

BY TCW CKD TJH

Alliant Burlington  
Economizer Ash Flow Estimate

1  
2 Economizer Pond Dam Break Problem

3  
4  $x = 2t\sqrt{g y_2} - 3t\sqrt{g y}$  <sup>eqn\*</sup> (19-62)  
5  
6

7  
8 Note: Initial Velocity = 0

9  
10  $y_2 =$  Initial Fluid Height = 18'  
11 (550' - 532')

12  
13  $x =$  distance of interest  
14 = distance to upper ash pond dike  
15 = 400'

16  
17 with  $x$  specified then  $y = f(t)$

18  
19 where  $y =$  depth @  $x$

20  
21  
22  $400' = 2\sqrt{g y_2} t - 3\sqrt{g y} t$

23  
24  
25  $3\sqrt{g y} = 2\sqrt{g y_2} - 400'/t$

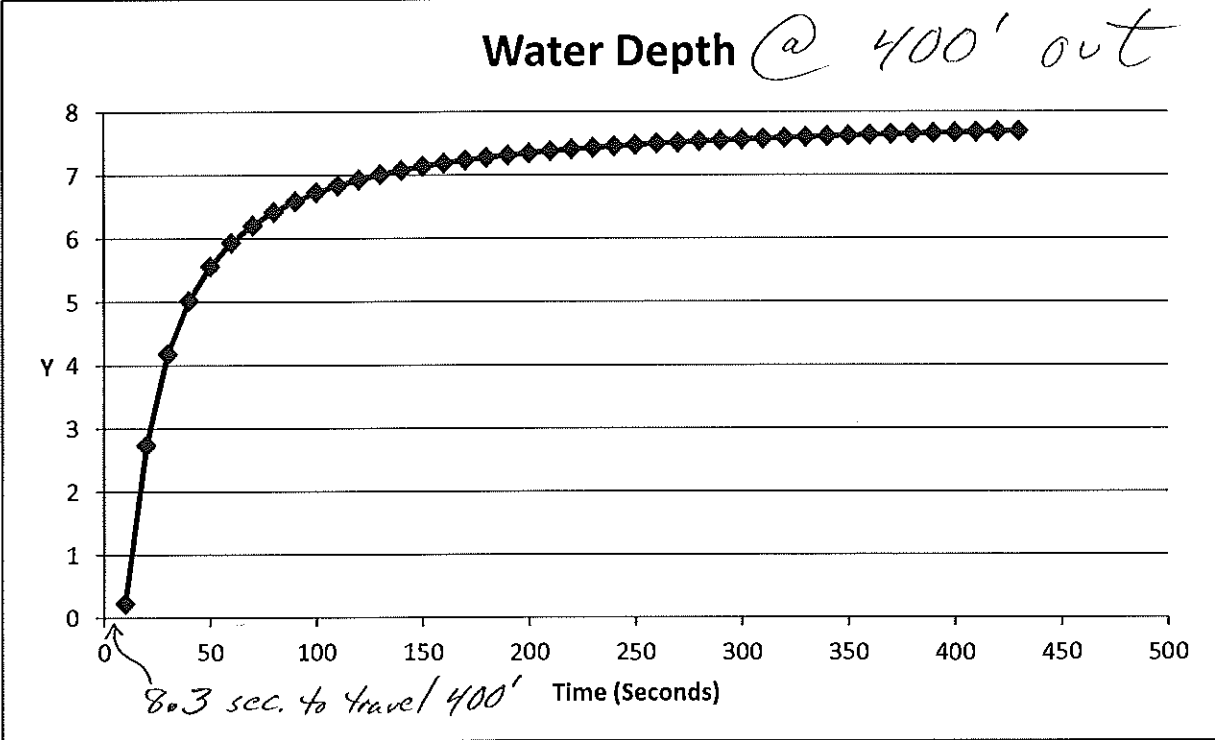
26  
27  
28  $y = \left( 2\sqrt{g y_2} - \frac{400'}{t} \right)^2 / (9g)$

29  
30  
31 if  $t \rightarrow \infty$  then  $y = 8'$  regardless of  $x$   
32 (given an infinite reservoir)

33  
34 \* Ref: Open Channel Hydraulics  
35 Chow 1959 p 568  
36

US EPA ARCHIVE DOCUMENT

Economizer Pond Dam-Break Problem



G            32.174 ft/sec<sup>2</sup>  
 Y0            18 ft  
 X            400 ft

t (sec.)	y (ft.)
10	0.22828
20	2.732762
30	4.181535
40	5.021037
50	5.561574
60	5.937281
70	6.213161
80	6.424182
90	6.590746
100	6.725532
110	6.836826
120	6.930269
130	7.009831
140	7.078389
150	7.138076
160	7.190507
170	7.236929
180	7.278319
190	7.315452
200	7.348952
210	7.379328

By TCW 3-22-2011  
 154.002.009  
 Alliant Energy - Burlington Generating Station  
 Ash Pond Stability

US EPA ARCHIVE DOCUMENT

6 1 1 1





SHEET NO. 3 OF 4

PROJECT NO. 154.002.009

DATE 3-22-11

BY TCW CKD TJH

Alliant Burlington  
ECONOMIZER ASH FLOW

1

2 wave front speed =  $2\sqrt{gh}$

3

4 = 48 fps = 33 mph

5

6 so 8.3 seconds to travel 400'

7 but height = zero on the leading edge

8

9  $Q_{max} = \frac{8}{27} \sqrt{g \cdot h}$  (eq. 1\*)

10

11

12  $V_{max} = \frac{2}{3} \sqrt{g \cdot h}$  (eq. 11\*)

13

14

15 where  $V_{max}$  is at the dam location

16

17  $\Rightarrow$  assume  $V_{max} = V_{max}$  at the dike

18 400 feet away

19

20  $V = 16.0$  fps

21

22 The pressure on the dike from such a

23 velocity can be calculated by

24

25  $p = \frac{1}{2} C_d \rho V^2$  (11.71\*\*)

26

27 ignoring hydrostatic forces

28

29  $\rho =$  mass of fluid

30

31 \*\* Ref; Earthquake Engineering, Robert L. Wigley

32 1970, p 299

33

34 \* Ref; Guidelines for Calculating and Routing a

35 Dam-Break Flood, USACE January 1977

36 RD-5

US EPA ARCHIVE DOCUMENT





SHEET NO. 4 OF 4  
PROJECT NO. 154.007.009  
DATE 3-22-11  
BY TOW CKD TSH

Alliant Burlington  
ECONOMIZER ASH FLOW

1	
2	$C_D = \text{drag coefficient}$
3	$= 1.0 \text{ for Equilateral Triangle}$
4	
5	
6	Ref: Applied Fluid Dynamics Handbook, Robert
7	D. Stevens, Ph.D. 1989, p 310
8	
9	$\rho = 95 \text{ PCF/g}$
10	
11	$p = \frac{1}{2} \cdot 1.0 \cdot \frac{95 \text{ PCF}}{322 \text{ fps}^2} (16 \text{ fps})^2$
12	
13	
14	
15	$= 380 \text{ PSF}$
16	
17	Acting on a eight foot high Dike/ft.
18	
19	$F = p \times H = 380 \text{ PSF} \times 8 \text{ ft}$
20	
21	$= 3,040 \text{ Pounds/ft width}$
22	
23	
24	Which is much less than the force required
25	to shear off the dike with its cohesion at
26	1,000 PSF +.
27	
28	
29	
30	
31	
32	
33	
34	
35	
36	

US EPA ARCHIVE DOCUMENT

CONFIDENTIAL BUSINESS INFORMATION

# OPEN-CHANNEL HYDRAULICS

VEN TE CHOW, Ph.D.

*Professor of Hydraulic Engineering  
University of Illinois*

McGRAW-HILL BOOK COMPANY

New York    Toronto    London

1959

US EPA ARCHIVE DOCUMENT

rs

cs

s

ete

where  $w$  is the unit weight of water,  $T$  is the top width, and  $h$  is the surge height. The kinetic energy of the element is evidently equal to

$$\text{K.E.} = \frac{wV^2yT}{2g} \tag{19-47}$$

where  $y$  is the depth of water and  $V$  is the velocity of flow. By Eq. (19-23) or Eq. (19-19), as the case may be, the above equation may be reduced to

$$\text{K.E.} = \frac{wh^2gyT}{2c^2} \tag{19-48}$$

Assuming a surge of small height,

$$c = \sqrt{gy}$$

and the above equation becomes

$$\text{K.E.} = \frac{1}{2}wh^2T \tag{19-49}$$

The total energy of surge per unit length is, therefore,

$$E = \text{P.E.} + \text{K.E.} = wh^2T \tag{19-50}$$

**19-4. Negative Surges.** Negative surges are not stable in form, because the upper portions of the wave travel faster than the lower portions (Art. 19-1). If the initial profile of the surge is assumed to have a

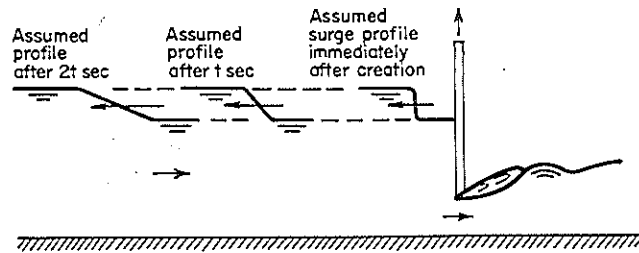


Fig. 19-8. Propagation of a negative surge due to sudden lift of a sluice gate.

step front, it will soon flatten out as the surge moves through the channel (Fig. 19-8). If the height of the surge is moderate or small compared with the depth of flow, the equations derived for a positive surge can be applied to determine approximately the propagation of the negative surge. If the height of the surge is relatively large, a more elaborate analysis is necessary as follows:

Figure 19-9 shows a type D surge (Fig. 19-2) of relatively large height, retreating in an upstream direction. The surge is caused by the sudden lifting of a sluice gate. The wave velocity of the surge actually varies from point to point. For example,  $V_w$  is the wave velocity at a point on the surface of the wave where the depth is  $y$  and the velocity of flow through the section is  $V$ . During a time interval  $dt$ , the change in  $y$  is  $dy$ . The value of  $dy$  is positive for an increase of  $y$  and negative for a decrease

of  $y$ . By the momentum principle, the corresponding change in hydrostatic pressure should be equal to the force required to change the momentum of the vertical element between  $y$  and  $y + dy$ . Considering a unit width of the channel and assuming  $\beta_1 = \beta_2 = 1$ ,

$$\frac{w}{2}y^2 - \frac{w}{2}(y + dy)^2 = \frac{w}{g}(y + \frac{1}{2}dy)(V + V_w)dV \tag{19-51}$$

Simplifying the above equation and neglecting the differential terms of higher order,

$$dy = -\frac{V + V_w}{g}dV \tag{19-52}$$

As described previously (Art. 19-1), the whole wavefront can be assumed to be made up of a large number of very small waves placed

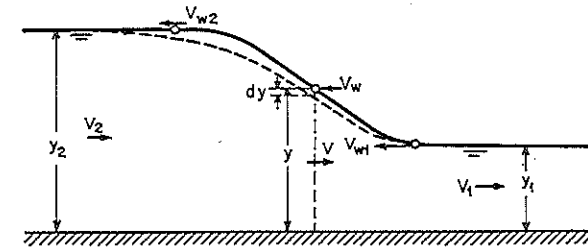


Fig. 19-9. Analysis of a negative surge.

one on top of the other. The velocity of the small wave at the point under consideration may be expressed according to Eq. (19-11) as

$$V_w = \sqrt{gy} - V \tag{19-53}$$

Similarly, the velocity at the wave crest is

$$V_{w2} = \sqrt{gy_2} - V_2 \tag{19-54}$$

and, at the wave trough,

$$V_{w1} = \sqrt{gy_1} - V_1 \tag{19-55}$$

When the surge is not too high, a straight-line relation between  $V_{w1}$  and  $V_{w2}$  may be assumed. Thus, the mean velocity of the wave may be considered to be

$$V_m = \frac{V_{w1} + V_{w2}}{2} \tag{19-56}$$

Now, eliminating  $V_w$  between Eqs. (19-52) and (19-53),

$$\frac{dy}{\sqrt{y}} = -\frac{dV}{\sqrt{g}} \tag{19-57}$$

Integrating this equation from  $y_2$  to  $y$  and from  $V_2$  to  $V$ , and solving for  $V$ ,

$$V = V_2 + 2\sqrt{gy_2} - 2\sqrt{gy} \tag{19-58}$$

From Eq. (19-53),

$$V_w = 3\sqrt{gy} - 2\sqrt{gy_2} - V_2 \tag{19-59}$$

Thus, the wave velocity at the trough of the wave is

$$V_{w1} = 3\sqrt{gy_1} - 2\sqrt{gy_2} - V_2 \tag{19-60}$$

Let  $t$  be the time elapsed since the surge was created or, in this case, since the sluice gate was opened. At  $t = 0$ , the wavelength  $\lambda = 0$ . After  $t$  sec, the wavelength is equal to

$$\lambda = (V_{w2} - V_{w1})t \tag{19-61}$$

The above analysis can be applied similarly to a negative surge of type C.

**Example 19-5.** Show that the equation of the wave profile, resulting from the failure of a dam is in the form of

$$x = 2t\sqrt{gy_2} - 3t\sqrt{gy} \tag{19-62}$$

where  $x$  is the distance measured from the dam site,  $y$  is the depth of the wave profile,  $y_2$  is the depth of the impounding water, and  $t$  is the time after the dam broke.

*Solution.* Since the impounding water has zero velocity, or  $V_2 = 0$ , the wave velocity by Eq. (19-59) is  $V_w = 3\sqrt{gy} - 2\sqrt{gy_2}$ . Since  $V_w$  is in the negative direction of  $x$ ,  $x = -V_w t$ , which gives Eq. (19-62).

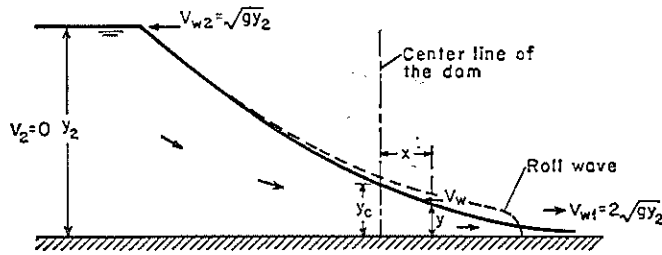


FIG. 19-10. Wave profile due to dam failure.

Equation (19-62) represents a parabola with vertical axis and vertex on the channel bottom, as shown in Fig. 19-10. At the site of the dam,  $x = 0$  and the depth  $y_c = 4y_2/9$ . Owing to the channel friction, the actual profile takes the form indicated by the dashed line. This profile has a rounded front at the downstream end, forming a bore (see Example 18-1). At the upstream end, the theoretical profile thus developed has been checked satisfactorily with experiments by Schoklitsch [12].

**19-5. Surge in Power Canals.** Engineers are interested in the determination of the maximum stage of water that could be developed as a

result of a sudden rejection of load in a power canal. This information is required in the design of the canal for establishing the height of wall necessary to prevent overflow.

Figure 19-11a shows the condition of steady flow in a power canal. The flow profile and the friction loss can be computed. When the load

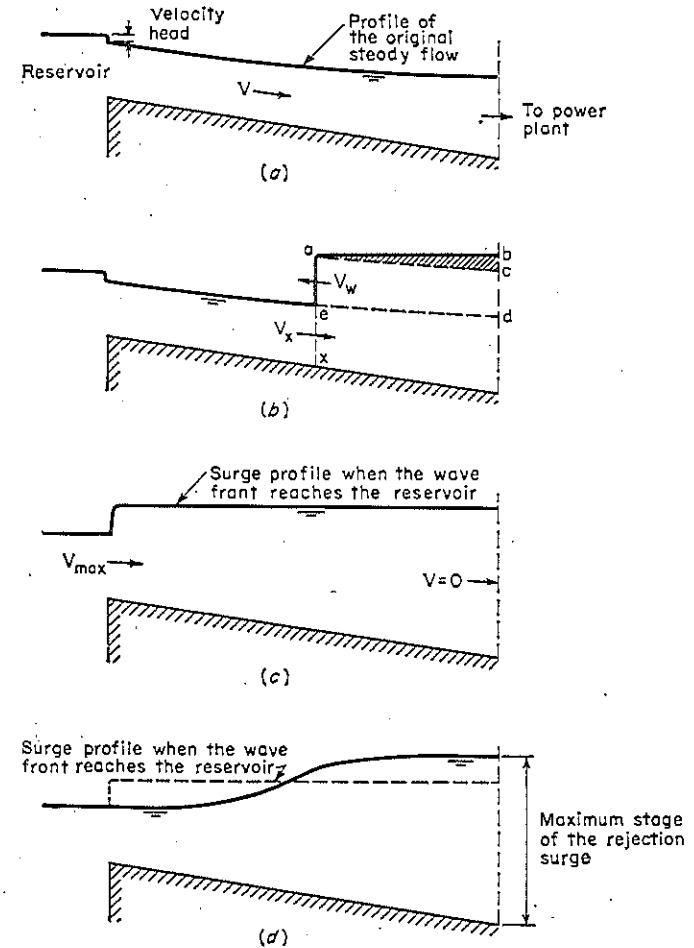
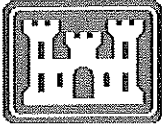


FIG. 19-11. Development of rejection surge in frictional channel.

is suddenly thrown off, a rejection surge advancing upstream is produced, as shown in Fig. 19-11b. According to usual observations, the water surface  $ab$  downstream from the wavefront is approximately level. Thus, when the wavefront reaches the reservoir, the water surface throughout the entire canal becomes level (Fig. 19-11c). However, a steadily



**US Army Corps  
of Engineers**  
Hydrologic Engineering Center

---

# **Guidelines for Calculating and Routing a Dam-Break Flood**

**January 1977**

**US EPA ARCHIVE DOCUMENT**



**CONFIDENTIAL BUSINESS INFORMATION**

**US EPA ARCHIVE DOCUMENT**

REPORT DOCUMENTATION PAGE			Form Approved OMB No. 0704-0188		
<p>The public reporting burden for this collection of information is estimated to average 1 hour per response, including the time for reviewing instructions, searching existing data sources, gathering and maintaining the data needed, and completing and reviewing the collection of information. Send comments regarding this burden estimate or any other aspect of this collection of information, including suggestions for reducing this burden, to the Department of Defense, Executive Services and Communications Directorate (0704-0188). Respondents should be aware that notwithstanding any other provision of law, no person shall be subject to any penalty for failing to comply with a collection of information if it does not display a currently valid OMB control number.  <b>PLEASE DO NOT RETURN YOUR FORM TO THE ABOVE ORGANIZATION.</b></p>					
1. REPORT DATE (DD-MM-YYYY) January 1977		2. REPORT TYPE Research Document		3. DATES COVERED (From - To)	
4. TITLE AND SUBTITLE Guidelines for Calculating and Routing a Dam-Break Flood				5a. CONTRACT NUMBER	
				5b. GRANT NUMBER	
				5c. PROGRAM ELEMENT NUMBER	
				5d. PROJECT NUMBER	
				5e. TASK NUMBER	
6. AUTHOR(S) David L. Gundlach, William A. Thomas				5f. WORK UNIT NUMBER	
7. PERFORMING ORGANIZATION NAME(S) AND ADDRESS(ES) US Army Corps of Engineers Institute for Water Resources Hydrologic Engineering Center (HEC) 609 Second Street Davis, CA 95616-4687				8. PERFORMING ORGANIZATION REPORT NUMBER RD-5	
9. SPONSORING/MONITORING AGENCY NAME(S) AND ADDRESS(ES)				10. SPONSOR/ MONITOR'S ACRONYM(S)	
				11. SPONSOR/ MONITOR'S REPORT NUMBER(S)	
12. DISTRIBUTION / AVAILABILITY STATEMENT Approved for public release; distribution is unlimited.					
13. SUPPLEMENTARY NOTES .					
14. ABSTRACT This report describes procedures necessary to calculate and route a dam-break flood using an existing generalized unsteady open channel flow model. The recent Teton Dam event was reconstituted to test the model's performance on such a highly dynamic wave. The procedures outlined relate, primarily, to require some further research and programming to improve the applicability of the program to dam-break flood events. The special project memo established four objectives for this study. The first two, (1) level of accuracy of existing techniques, and (2) sensitivity of calculated results to n-values and breach size, were summarized and presented in detail in Appendix A of this document. The third objective, (3) description of physical phenomena controlling depth and travel time and a discussion of pertinent field data, was presented in the body of this report. The fourth objective, (4) documentation of the methodology, was included in Appendix B of this document. Computer programs utilized in the methodology may be obtained from the Hydrologic Engineering Center. The computer program was applied to the Teton Dam data set to demonstrate the level of accuracy one might expect in such analyses. The results were shown and, in general, appear reasonable.					
15. SUBJECT TERMS dam failure ,flood profiles, model studies, waves (water), open channel flow, flood routing, mathematical models, analytical techniques, analysis, hydrographs, hydrograph analysis, water levels, discharge (water), reservoirs, peak discharge, rupturing, unsteady flow, steady flow, Teton Dam					
16. SECURITY CLASSIFICATION OF:			17. LIMITATION OF ABSTRACT UU	18. NUMBER OF PAGES 64	19a. NAME OF RESPONSIBLE PERSON
a. REPORT U	b. ABSTRACT U	c. THIS PAGE U			19b. TELEPHONE NUMBER



# Guidelines for Calculating and Routing a Dam-Break Flood

January 1977

US Army Corps of Engineers  
Institute for Water Resources  
Hydrologic Engineering Center  
609 Second Street  
Davis, CA 95616

(530) 756-1104  
(530) 756-8250 FAX  
[www.hec.usace.army.mil](http://www.hec.usace.army.mil)

RD-5

## CONFIDENTIAL BUSINESS INFORMATION

### FOREWORD

This Research Note reports the findings of The Hydrologic Engineering Center on appropriate methodologies for calculating and routing floods resulting from suddenly-breached dams.

This study was prepared for the U.S. Army Engineer Waterways Experiment Station, Vicksburg, Miss. with funding provided by the Defense Nuclear Agency under subtask L19HAXSX337, "Above Ground Structures," work unit 07, "Damage of Dams," and by the Office, Chief of Engineers under DA project 4A762719AT40, task A1, work unit 006.

The material contained herein is offered for information purposes only and should not be construed as Corps of Engineers policy or as being recommended guidance for field offices of the Corps of Engineers.

CONFIDENTIAL BUSINESS INFORMATION

GUIDELINES FOR  
CALCULATING AND ROUTING A DAM-BREAK FLOOD

Table of Contents

<u>Paragraph</u>	<u>Page</u>
1. Introduction	1
2. Summary	2
3. Physical Phenomena and Field Data	3
4. Energy Components and Peak Outflow from Complete, Instantaneous Breaches	5
5. Instantaneous, Partial Breaches	6
6. Attenuation of the Flood Wave	9
7. Proposed Analytical Technique	9
8. Program Limitations	10
9. Proposed Areas of Research	11
10. Alternate Analytical Procedures	11
11. References	12

CONFIDENTIAL BUSINESS INFORMATION

LIST OF TABLES

<u>Table</u>	<u>Page</u>
1 Sensitivity to Breach Size and Rate of Development	2
2 Relative Size of Energy Components in Partial Width Breaches	8

LIST OF FIGURES

<u>Figure</u>	<u>Page</u>
1 Components of Specific Energy Head	6

CONFIDENTIAL BUSINESS INFORMATION

APPENDICES

APPENDIX A

Unsteady Flow Analysis - Teton Dam Failure

Table of Contents

<u>Paragraph</u>	<u>Page</u>
1. Introduction	A-1
2. General Description	A-1
3. Geometric Models	A-2
4. Unsteady Flow Models	A-5
5. Steady Flow Model	A-15



CONFIDENTIAL BUSINESS INFORMATION

LIST OF TABLES

<u>Table</u>	<u>Page</u>
1 Estimated Times for Leading Edge of Flood Wave	A- 3
2 Estimated Peak Discharges	A- 4
3 Results of Unsteady Flow Analysis Using Simulated Discharge Hydrograph for Observed Conditions	A- 8
4 Computed and observed Times for Leading Edge of Flood Wave	A-10
5 Computed and Observed Peak Discharges	A-11
6 Results of Unsteady Flow Analysis Using Simulated Discharge Hydrograph for 40% Breach Size	A-12

# CONFIDENTIAL BUSINESS INFORMATION

## LIST OF PLATES

<u>Plate</u>	<u>Page</u>
1 Teton Dam, Teton River, Idaho Location Map	A-16
2 Teton Dam General Plan and Sections	A-17
3 Teton Dam Embankment Details	A-18
4 Teton Dam Reservoir Capacity	A-19
5 Teton Dam Elevation Hydrograph for Reservoir	A-20
6 Teton Dam Discharge Hydrograph at Damsite	A-21
7 Teton Dam initial Estimate of Partial Failure	A-22
8 Teton Dam Estimate of Partial Failure	A-23
9 Teton Dam Discharge Hydrographs at Damsite	A-24
10 Teton Dam Flooded Area Map Including High Water Marks	A-25
11 Teton Dam Maximum Computed Water Surface Elevations for June 5, 1976 Dam Failure	A-26
12 Teton Dam Maximum Computed Water Surface Elevations for June 5, 1976 Dam Failure	A-27
13 Teton Dam Maximum Computed Water Surface Elevations for June 5, 1976 Dam Failure	A-28
14 Teton Dam Computed Times for June 5, 1976 Dam Failure	A-29
15 Teton Dam Maximum Computed Water Surface Elevations for June 5, 1976 Dam Failure	A-30
16 Teton Dam Maximum Computed Water Surface Elevations for June 5, 1976 Dam Failure	A-31
17 Teton Dam Maximum Computed Water Surface Elevations for June 5, 1976 Dam Failure	A-32

CONFIDENTIAL BUSINESS INFORMATION

APPENDIX B

Guidelines for Analyzing a Dam Break Flood with the Computer Program  
"Gradually Varied Unsteady Flow Profiles"

Table of Contents

<u>Paragraph</u>	<u>Page</u>
1. Data Requirements	B-1
2. Assumptions	B-1
3. General Procedure	B-2
4. Calculation of Outflow Hydrograph Using the Partial Breach Approach	B-2
5. Routing the Dam Break Flood	B-3

# CONFIDENTIAL BUSINESS INFORMATION

## RESEARCH NOTE NO. 5

### GUIDELINES FOR CALCULATING AND ROUTING A DAM-BREAK FLOOD

1. Introduction. Planning and design requirements for a wide range of projects, such as emergency preparedness and siting of nuclear power plants, have generated widespread interest in dam break floods. Much academic research and some laboratory research have been accomplished on this topic. Generalized analytic techniques for calculating and routing such floods, particularly in non-prismatic valleys, have not been readily available. Furthermore, prototype verification data are almost non-existent. This report describes procedures necessary to calculate and route a dam break flood using an existing generalized unsteady open channel flow model. The recent Teton Dam event was reconstituted to test the model's performance on such a highly dynamic wave. The procedures outlined herein relate, primarily, to partial breaches. Some deficiencies in the model were identified which will require some further research and programming to improve the applicability of the program to dam break flood events.

2. Summary. The special projects memo cited as reference (a) established four objectives for this study. The first two, a) level of accuracy of existing techniques and b) sensitivity of calculated results to n-values and breach size, are summarized below and presented in detail in Appendix A. The third objective, c) description of physical phenomena controlling depth and travel time and a discussion of pertinent field data, is presented in the body of this report. The fourth objective, d) documentation of the methodology, is included in Appendix B. Computer programs utilized in the methodology, references (b) and (c), may be obtained from The Hydrologic Engineering Center.

The computer program of reference (c) was applied to the Teton Dam data set to demonstrate the level of accuracy one might expect in such analyses. The results are shown on pages A-26 through A-28 of Appendix A and, in general, appear reasonable. This test case demonstrates the usefulness of a generalized computer program because the methods proposed in references (d) and (e) were not applicable to the Teton data set for reasons given in paragraph 10.

**CONFIDENTIAL BUSINESS INFORMATION**

Regarding sensitivity to breach size, pages A-22 and A-23 show the two breach sizes considered. The breach that developed at Teton was estimated, by others, to be 40 percent of the dam embankment. Geometric data were not available to verify this, therefore, our best estimate of the final Teton breach geometry, page A-22, is based on photographs. The breach shown on page A-23 has the same side slope as that on page A-22, 0.6 on 1, but it has zero bottom width. This seemed a likely intermediate condition, but no field data were available at the time of this study to establish an observed intermediate condition.

The calculated outflow is shown on page A-24. The hydrograph labeled "trapezoidal breach" assumed the 40 percent breach size, page A-22, developed instantaneously. The hydrograph labeled "triangular breach" was determined in a similar manner for the 30% breach size. The third hydrograph on page A-24 was calculated for the trapezoidal breach (labeled 40% breach size on page A-22), but an observed reservoir drawdown curve at the dam, page A-20, was used which implies a gradual development of the breach rather than instantaneous failure. The last approach was considered best in estimating the discharge hydrograph from Teton reservoir given the data set and analytical techniques available to us.

The sensitivity of calculated outflows to breach size and rate of development is illustrated on page A-24. It is summarized in the following table together with pertinent elevation data for an n value of 0.04.

Table 1: Sensitivity to Breach Size and Rate of Development

Final Breach Size % of Total Dam	Rate of Development	Calculated Peak Water Discharge at Dam Axis 10 <sup>6</sup> CFS (1)	Calculated Peak Elevations		
			MSL		
			At Dam Axis	Miles Downstream from Dam Axis	
				5	10
40%	(2)	1.8 (3)	5123	5014	4933
30%	instantaneous	2.4	5151	5015	4933
40%	instantaneous	3.4	5175	5020	4935

- (1) Multiply by 0.02832 to get Cubic Meters Per Second
- (2) Actual rate of development was unknown so the observed reservoir drawdown curve, page A-20, was used to approximate outflow conditions.

## CONFIDENTIAL BUSINESS INFORMATION

- (3) The actual peak discharge, as estimated by personnel of the Walla Walla District, Army Corps of Engineers from observed data in the Teton Canyon three miles downstream from the dam, was 2,300,000 cfs.

From these results it is apparent that neither the size of breaches tested nor the rates of failure assumed were very significant in predicting peak elevations five miles downstream from the dam.

The calculated peak flood elevations, near the dam, were very sensitive to n-values. Increasing n from .03 to .06 raised the peak flood elevation 25 feet at the dam, as illustrated on page A-8, Table 3. At 5 miles downstream the calculated difference was only 8 feet. Differences continued to diminish with distance.

Calculated Travel Times are shown on page A-29. They correspond to the discharge hydrograph labeled "simulated from observed data" on page A-24 and n-values of 0.04.

Searching for a simplified approach in place of references (d) and (e) led to a trial application of the Modified Puls routing technique. The hydrograph labeled "simulated from observed data" on page A-24 was routed and a water surface profile calculated for the resulting peak discharges. A comparison of the results with the observed elevations and the peak elevations computed with the full equations is shown on pages A-30 through A-32. Additional investigation is needed to establish the range of applicability of this method.

3. Physical Phenomena and Field Data. Analysis of the dam-break flood involves understanding the physical processes before applying analytical techniques which approximate those physical processes. Three distinctly different processes are involved: the process of structural failure causing the breach to develop; the process of setting water into motion in a reservoir; and the process of flood wave attenuation.

The size, shape and rate of breach development are primarily responsible for the peak rate of outflow from the reservoir. Yet, of the three physical processes, this one is the most difficult to quantify. With the exception of man-made breaches, it is difficult to visualize the instantaneous development of a breach. Some have occurred, however. The St. Frances Dam, a high head concrete gravity structure, apparently suffered an abutment failure which resulted in virtually the instantaneous failure of the entire structure. The Johnstown flood of 1889 was caused by the complete failure of an earth fill dam. Reports indicate that less than half an hour was required for overtopping flow to breach the structure. The recent Teton failure, a full depth-partial width breach of an earth fill dam, is estimated to have developed in less than two hours. Since natural failure of a major structure is so improbable, establishing a mode of failure requires a policy decision rather than an analytical technique. In general, instantaneous failure of the entire structure produces the largest flood wave.



## CONFIDENTIAL BUSINESS INFORMATION

The second physical process results from the depth of water above the breach invert. That is, a reservoir has a total energy head equal to the elevation of the water surface. If the dam is breached, the force of gravity will set water into motion. The effect will propagate, as a negative wave, to the upstream end of the reservoir at a velocity equal to  $\sqrt{gy}$  where  $g$  is acceleration of gravity and  $y$  is water depth. Because of the great depth in a reservoir, very little frictional resistance is mobilized during the passage of this negative wave. As a result, water gains specific energy rapidly as it moves toward the breach. In instantaneous breach development, the peak outflow will occur within a minute or two after breaching.

Whereas the total energy head setting the water into motion is the specific energy (i.e., the initial water depth) above the breach invert, the energy which must be dissipated in the downstream channel is equal to the specific energy from the downstream channel invert to the initial pool elevation. The fact that the water surface elevation drops down rapidly at the dam axis does not reflect a corresponding loss in energy head. When flow begins, that specific energy above the breach invert is transformed into three components: a pressure head, a kinetic energy head and an inertia head. (The relative size of each of these energy head components is discussed more fully in sections 4 and 5.) Friction loss is relatively small and may be neglected unless the reservoir bottom is extremely rough (more than 5% or 10% of the water depth).

The third physical process, flood wave attenuation, involves energy dissipation and valley storage. As the flood wave moves downstream, the peak discharge tends to decrease, the base of the flood wave will become longer and the wave velocity will decrease. Near the dam, energy dissipation is primarily responsible for behavior of the flood wave. However, valley storage soon becomes the primary factor in flood wave attenuation. The key to the transition from energy dissipation to valley storage control is the rate at which the slope of the total energy gradient, a line which must intersect the initial pool elevation at the dam, is reduced to that of a major rainfall flood in the downstream valley. It seems obvious that the total energy at any cross section in the valley should not exceed the initial reservoir elevation, and yet some analytical techniques occasionally violate that constraint. It is good policy to always check the total energy, as well as the water volume, in a calculated flood wave.

The rate of energy dissipation is governed primarily by friction loss. Minor losses from bends and contractions-expansions are often included in the  $n$ -values.

The volume of water in the reservoir is the final piece of field data required. This volume strongly influences the peak elevations at downstream points.

CONFIDENTIAL BUSINESS INFORMATION

4. Energy Components and Peak Outflow from Complete, Instantaneous Breaches. It is useful to develop the relative size for each energy component in the flow at the dam axis and to compare all of them to the more common case of steady state critical flow at a contraction.

By assuming a rectangular cross section, zero bottom slope and instantaneous removal of the entire dam, Saint-Venant developed an analytical solution for the elevation of the free surface, reference (f), page 755. Utilizing that equation, the depth of flow at the dam axis was determined, by Saint-Venant and others, to be  $\frac{4}{9} Y_0$  where  $Y_0$  is the original water depth at the dam. Also, the velocity corresponding to the peak outflow was shown to be  $\frac{2}{3} \sqrt{gY_0}$ . Combining these relationships leads to the equation for peak discharge

$$q_{max} = \frac{8}{27} Y_0 \cdot \sqrt{g \cdot Y_0} \tag{1}$$

- $Y_0$  is the initial water depth at the dam
- $g$  is acceleration of gravity
- $q_{max}$  is peak water discharge in cfs/ft

Since this equation was developed for a rectangular section, the total discharge may be calculated by multiplying  $q_{max}$  by the width.

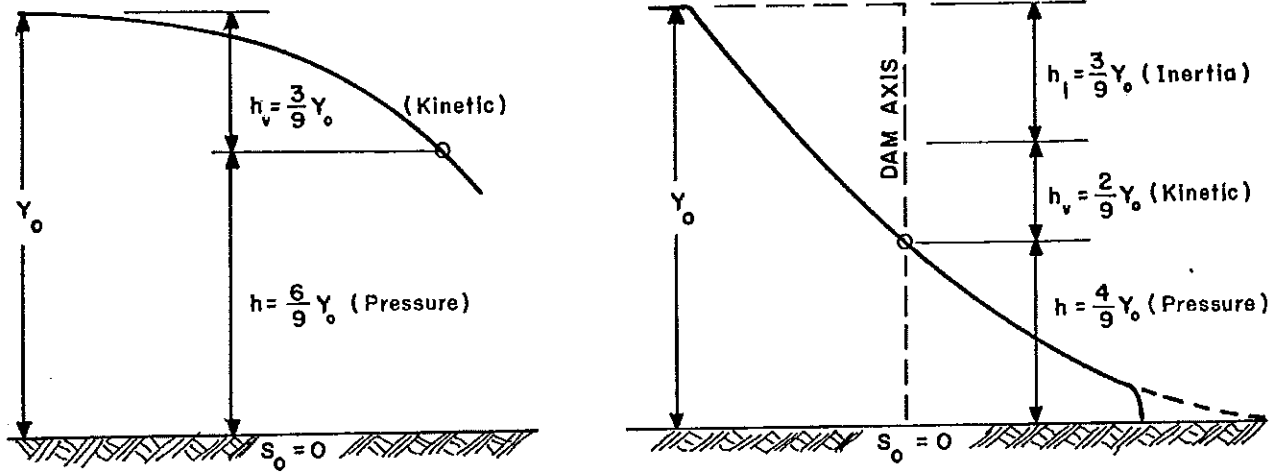
Using the relationships referenced above, the velocity head (i.e., the kinetic energy head component of the specific energy head) was calculated to be  $\frac{2}{9} Y_0$ . Since, in the absence of friction and other losses, inertia is the only remaining term in the basic, unsteady flow equations of Saint-Venant, it may be calculated as follows.

$$Y_0 = h_i + \frac{2}{9} Y_0 + \frac{4}{9} Y_0 \tag{2}$$

$$h_i = \frac{3}{9} Y_0$$

These components are shown in Figure 1 along with the energy components for critical, steady state flow.

This figure shows that in the dam break flood analysis, as well as steady state critical flow at a contraction, the velocity head is half the pressure head. However, the inertia head component is zero in Figure 1a because flow is steady state.



(a) Critical flow at a contraction (steady flow conditions)

(b) Critical flow from a breached dam (unsteady flow conditions)

Figure 1. Components of Specific Energy Head.

The drawdown in water surface elevation to  $\frac{4}{9} Y_0$  at the dam axis, Figure 1b, does not reflect a corresponding energy loss. Experimental results obtained by Schoklitsch, reproduced on page 755 of reference 1f, show relatively little friction loss in flow approaching the dam axis. As might be expected, the model results showed friction to be very significant downstream. Tests reported by WES in reference (g) showed no impact from friction loss at the dam axis. However, the WES flume sloped at 0.005 ft/ft, whereas the flume in Schoklitsch's experiment had zero bottom slope.

The significance of this point is that all three energy components, pressure head, kinetic energy head and inertia head, are significant in complete, instantaneous breaches. Consequently, investigators encourage the use of the complete routing equations, often referred to as the Saint-Venant equations. Simplifications of the complete equations, such as Muskingham, Tatum, Straddle-Stagger and Modified Puls, are not recommended because the empirical coefficients would invariably be developed from rainfall floods and would reflect different values of energy components relative to  $Y_0$ .

5. Instantaneous, Partial Breaches. Partial breaches are classified, according to hydraulic performance, as full depth-partial width, partial depth-full width or partial depth-partial width. A separate equation has been developed for calculating the peak water discharge for each class, page 25 of reference (g).

CONFIDENTIAL BUSINESS INFORMATION

Full Depth-Partial Width

$$Q_{\max} = \frac{8}{27} \cdot b \cdot Y_0 \cdot \left(\frac{B}{b}\right)^{\frac{1}{4}} \sqrt{gY_0} \quad (3)$$

B is width of channel, feet  
b is width of breach, feet

Partial Depth-Full Width

$$Q_{\max} = \frac{8}{27} \cdot B \cdot y \left(\frac{Y_0}{y}\right)^{\frac{1}{3}} \sqrt{gy} \quad (4)$$

y is depth of water above bottom of breach

Partial Depth-Partial Width

$$Q_{\max} = \frac{8}{27} \cdot b \cdot y \cdot \left(\frac{B}{b}\right)^{\frac{1}{4}} \cdot \left(\frac{Y_0}{y}\right)^{\frac{1}{3}} \sqrt{gy} \quad (5)$$

An empirical equation for partial depth-partial width breaches was reported in references (g) and (h).

$$Q_{\max} = 0.29 \cdot b \cdot y \cdot \left(\frac{B}{b} \cdot \frac{Y_0}{y}\right)^{0.28} \cdot \sqrt{gy} \quad (6)$$

For breach sizes in the following range.

$$1 \leq \left(\frac{B}{b} \cdot \frac{Y_0}{y}\right) \leq 20 \quad (7)$$

Since the discharge equations for partial breaches are similar, in form, to that for a full breach (1), the total specific energy has the same three basic components. However, their size, relative to initial water depth, is considerably different from that shown in Figure 1. There is no analytical solution for partial breaches, therefore, experimental results, presented in reference(g), were used to calculate the individual energy head components. The following table presents experimental results for full depth breaches ranging in width from 10% to 100% of the flume width in columns 1, 2 and 3. Fractions of initial water depth, calculated with equation 3, are shown in columns 4 and 5. A sample of the calculations is presented in the paragraph following the table. This sample calculation utilizes equation 3 and a 100% breach size (i.e., full breach) to demonstrate that the relative value of each energy component is the same as the respective value produced by equation 1, the analytical, full breach equation, when equation 3 is carried to its upper limit.

**CONFIDENTIAL BUSINESS INFORMATION**

Table 2: Relative Size of Energy Components in Partial Width Breaches<sup>(1)</sup>

Test No	Breach Size %	Pressure Head % of $Y_0$	Velocity Head (2) % of $Y_0$	Inertia Head (3) % of $Y_0$
(1)	(2)	(3)	(4)	(5)
1.1	Full	44	22	34
2.1	60	70	12	18
3.1	30	82	12	6
4.1	15	89	(4)	--
5.1	10	94	(4)	--

- Notes: 1. Values in columns 1 and 2 are from Table A, page 8, reference (g) and values in column 3 are from experimental results from Tables 1 through 5, Station 200, reference (g).
2. Velocity head is calculated with equations 8 and 9, following.
3. Inertia head is  $Y_0 - (\text{pressure head} + \text{velocity head})$ .
4. Calculated values exceeded 100 percent of  $Y_0$ , which probably reflects scatter in experimental results.

$$v_{\max} = \frac{Q_{\max}}{b \cdot y} \tag{8}$$

where:

$y$  = depth of water at dam axis

$b$  = breach width

$Q_{\max}$  from equation (3)

$$v_{\max} = \frac{\frac{8}{27} \cdot b \cdot Y_0 \left(\frac{B}{b}\right)^{\frac{1}{4}} \sqrt{gY_0}}{b \cdot y} \tag{9}$$

For the full breach,  $b = 1.0B$  and  $y = \frac{4}{9} Y_0$

CONFIDENTIAL BUSINESS INFORMATION

$$V_{\max} = \frac{\frac{8}{27} \cdot Y_0 \left(\frac{B}{1.0B}\right)^{\frac{1}{4}} \sqrt{gY_0}}{\frac{4}{9} \cdot Y_0} \quad (10)$$

$$V_{\max} = \frac{2}{3} \sqrt{gY_0} \quad (11)$$

$$\frac{V_{\max}^2}{2g} = \frac{4}{9} \frac{gY_0}{2g} \quad (12)$$

$$= \frac{2}{9} Y_0 \quad (13)$$

This agrees with section 4 and shows the procedure followed in completing Table 2. The inertia head, column 5 in Table 2, was calculated assuming zero energy loss upstream from the dam.

$$Y_0 = h_i + \frac{2}{9} Y_0 + \frac{4}{9} Y_0 \quad (14)$$

$$h_i = \frac{3}{9} Y_0 \quad (15)$$

Because of the decrease in relative significance of inertia head and even velocity head, it is satisfactory to apply simplifications of the full Saint-Venant equations to partially breached dams.

6. Attenuation of the Flood Wave. As a flood wave moves downstream, friction and other losses change the relative size of the three energy components. Even floods from fully breached dams eventually take on the characteristics of a rainfall flood and may be routed with a simplified routing method such as Modified Puls. Major areas of uncertainty are 1) how much distance is required for this transition, 2) how does this distance vary when considering partial breaches and 3) what is the maximum breach size to consider as a partial breach.

7. Proposed Analytical Technique. The guidelines presented in Appendix B of this report are developed for the computer program "Gradually Varied Unsteady Flow Profiles". It is a solution of the basic Saint-Venant equations for unsteady flow and may be used to calculate the outflow hydrograph through any size or shape of breach, as well as to route that hydrograph downstream and provide water discharge and water surface elevation



## CONFIDENTIAL BUSINESS INFORMATION

hydrographs at any number of computation points up to 45. The maximum discharge, maximum elevation and maximum flow velocity are summarized for each computation point.

Sufficient information is printed out so the time of arrival, time of peak and duration of the flood may be plotted.

This computer program accounts for the movement of the negative wave through the reservoir, for the tailwater submergence at the dam, for the three components of energy presented earlier, for friction loss and for storage in the reservoir and the downstream valley.

Cross sections need not be rectangular or prismatic. A companion program, "Geometric Elements from Cross Section Coordinates", is available to transform complex cross sections into the required geometric data set for the routing program.

These computer programs are generalized. That is, they are sufficiently flexible and adaptable to be used without code changes. They are portable from one computer to another and documentation is available, from The Hydrologic Engineering Center.

### 8. Program Limitations.

a. Routing with the Gradually Varied Unsteady Flow Profiles computer program requires a large high speed computer (50,000, 60-bit words) and personnel who are experienced in applying mathematical models.

b. Any breach size may be modeled, but the program assumes instantaneous development.

c. All channels must be wet initially. That is, computations cannot be made if any portion of the model is dry. This is overcome by prescribing a base flow; however, the computer program has difficulty in establishing this profile.

d. Movement of the negative wave through the reservoir causes no computational problem until it reaches the upstream end of the reservoir. Computation nodes tend to go dry and abort the computer run.

e. The analysis of multiple failures would require manual intervention to stop and restart the calculation process as each new structure is brought into the system.

f. The program assumes a horizontal water surface transverse to the flow, whereas a great deal of transverse slope can exist in the actual prototype situation.

## CONFIDENTIAL BUSINESS INFORMATION

9. Proposed Areas of Research. All of the program limitations were circumvented in analyzing the Teton Data Set. The trade-off, however, was analysis time. Seven weeks were required to set up the data, debug it and perform the analysis. The two tasks requiring the most time, probably 75%, were establishing initial base flow conditions for the model (8c) and stabilizing the computations when the negative surge reached the upstream boundary (8d). Both of these problem areas can be overcome by additional programming. The improvements would reduce analysis time to four or five weeks.

Instantaneous breach development, 8b, could be replaced by equations which let progressive development take place. In the absence of a theory, the rate of development would have to be prescribed with input data.

Developing the capability to handle multiple dam failures (8e), especially in tandem, will be a major modification.

This analytical technique is a one-dimensional model and will always have a horizontal water surface transverse to the flow. At present, two-dimensional modeling is not feasible.

10. Alternate Analytical Procedures. Alternate analytical procedures were proposed in references (d) and (e). Neither were applicable to the Teton Data Set.

The dimensionless curves were developed from numerical solution of the St. Venant equations and include special treatment of the wave front as it moves along a dry channel. By knowing reservoir volume, valley cross section at the dam, initial reservoir elevation, stream slope and stream roughness, the curves will provide three properties of the flood wave:

1. Time of arrival at downstream points
2. Maximum depth profile in the downstream channel
3. Time of maximum depth at downstream points.

The curves extend for distances ranging up to fifteen times the reservoir length. The outflow hydrograph at the dam is not needed to use these curves. It was assumed, in developing the curves, that the entire dam is breached instantaneously and that the valley is prismatic. Neither condition was satisfied by the Teton case.

The procedure in reference (e) was developed for smaller structures and the Teton Data Set was completely beyond the range of nomographs and curves presented there. In any case, the procedure does not route the flood wave downstream. Only the outflow discharge hydrograph is calculated at the dam axis. The procedure can handle a wide range of breach sizes, but it

## CONFIDENTIAL BUSINESS INFORMATION

is designed with partial breaches in mind. It has the advantage of tail water correction, which is essential when breaching of a low dam coincides with a high flow condition in the stream. The procedure is well documented and is easily applied.

A possible alternative approach for partial breaches is the Modified Puls routing technique. Preliminary work with this technique produced the results shown on pages A-30 through A-32 for the Teton Data Set. A Manning  $n$  value of 0.04 was used; further details are given in Paragraph 5, Appendix A. The advantage of this technique is that readily available and easily applied computer programs (e.g., HEC-1 and HEC-2) can be utilized; total analysis time would probably be reduced to two to three weeks.

The disadvantage is that the range of application is limited whereas the technique presented in Paragraph 7 is generally applicable.

Additional research is needed to define the range of applicability of the Modified Puls technique. The present hypothesis is that the size of the inertia component, Table 2, would provide a suitable parameter for defining that range.

This research would not require additional physical modeling. Studies reported in references (g) and (h) offer test data for numerical studies. Other numerical experiments could be performed by using results from analyzing variations of the Teton Data Set with the complete equations. These results could be obtained while pursuing any of the areas of research proposed in Section 9.

Computer programs which utilize the Modified Puls routing technique are available and are presently developed to a higher degree of serviceability than programs solving the full equations. Water surface profile computations will be required in conjunction with the Modified Puls routing to produce a water surface profile. These computations are computerized also. No major computer program development would be required. The appropriate existing computer programs, HEC-1 and HEC-2, are well documented.

### 11. References.

- a. Special Projects Memo No. 473 subject Calculating and Routing the Flood Resulting from a Suddenly Breached Dam, dated 26 August 1976.
- b. "Geometric Elements from Cross Section Coordinates", The Hydrologic Engineering Center, June 1976.
- c. "Gradually Varied Unsteady Flow Profiles", The Hydrologic Engineering Center, June 1976.
- d. "Dimensionless Graphs for Routing Floods from Ruptured Dams", by John Sakkas, dated January 1976, The Hydrologic Engineering Center.

CONFIDENTIAL BUSINESS INFORMATION

e. "Computation of Outflow from Breached Dams", Defense Intelligence Agency, June 1963.

f. Keulegan, G.H., "Wave Motion", Engineering Hydraulics, Ed. by H. Rouse, John Wiley & Sons, Inc., New York, New York, Fifth Printing, October 1965.

g. "Flood Resulting From Suddenly Breached Dams", Conditions of Minimum Resistance, Hydraulic Model Investigation, Miscellaneous Paper No. 2-374, Report 1, U.S. Army Corps of Engineers, Waterways Experiment Station, Vicksburg, Mississippi, February 1960.

h. "Floods Resulting From Suddenly Breached Dams", Conditions of High Resistance, Hydraulic Model Investigation, Miscellaneous Paper No. 2-374, Report 2, U.S. Army Corps of Engineers, Waterways Experiment Station, Vicksburg, Mississippi, November 1961.

CONFIDENTIAL BUSINESS INFORMATION

# EARTHQUAKE ENGINEERING

**ROBERT L. WIEGEL**

**Coordinating Editor**

**PRENTICE-HALL, INC., Englewood Cliffs, N. J.**

US EPA ARCHIVE DOCUMENT

CONFIDENTIAL BUSINESS INFORMATION

© 1970 by PRENTICE-HALL, INC., Englewood Cliffs, N.J.

All rights reserved. No part of this book may be reproduced in any form or by any means without permission in writing from the publisher.

Current printing (last digit):

19 18 17 16 15 14 13 12 11

13-222646-4

Library of Congress Catalog Card Number 75-76876

Printed in the United States of America

PRENTICE-HALL INTERNATIONAL, INC., *London*  
PRENTICE-HALL OF AUSTRALIA, PTY. LTD., *Sydney*  
PRENTICE-HALL OF CANADA, LTD., *Toronto*  
PRENTICE-HALL OF INDIA PRIVATE LTD., *New Delhi*  
PRENTICE-HALL OF JAPAN, INC., *Tokyo*

- 9 EARTHQUAKE DAMAGE AND STRUCTURAL PERFORMANCE IN THE UNITED STATES, 167**  
Karl V. Steinbrugge
- 9.1 Introduction, 167. 9.2 Definition and discussion of terms, 168. 9.3 Seismic risk, 170. 9.4 Case histories, 171. 9.5 Surface faulting, 223.*
- 10 SOIL PROBLEMS AND SOIL BEHAVIOR, 227**  
H. Bolton Seed
- 10.1 Introduction, 227. 10.2 Settlement of cohesionless soils, 228. 10.3 Soil liquefaction—level ground, 229. 10.4 Soil liquefaction in sloping ground—flow slides, 233. 10.5 Waterfront bulkhead failures due to backfill liquefaction, 234. 10.6 Slides caused by liquefaction of thin sand layers, 237. 10.7 Landslides in clay soils, 239. 10.8 Sloping fills on firm foundations, 243. 10.9 Sloping fills on weak foundations, 243. 10.10 Canal banks, reservoirs, and earth dams, 245. 10.11 Retaining walls and bridge abutments, 246. 10.12 Conclusion, 247.*
- 11 TSUNAMIS, 253**  
Robert L. Wiegel
- 11.1 Causes and nature of tsunamis, 253. 11.2 Damage by tsunamis, 260. 11.3 Theory and laboratory studies of tsunami generation, 264. 11.4 Travel of tsunamis in the ocean, 275. 11.5 Tsunami waves along the shore, 280. 11.6 Distribution of run-up elevations and wave heights along a coast, 288. 11.7 Tsunami distribution functions, 294. 11.8 Overtopping of seawall, 297. 11.9 Tsunami wave forces, 299.*
- 12 EARTHQUAKE RESPONSE OF STRUCTURES, 307**  
Ray W. Clough
- 12.1 Introduction, 307. 12.2 Single-degree-of-freedom systems, 310. 12.3 Multidegree-of-freedom systems, 322. 12.4 Nonlinear earthquake response, 328.*
- 13 APPLICATIONS OF RANDOM VIBRATION THEORY, 335**  
Joseph Penzien
- 13.1 Introduction, 335. 13.2 The random process, 336. 13.3 Effect of random process on systems, 337. 13.4 Elastic response of the single-degree system to random inputs, 338. 13.5 Applications in earthquake engineering, 340.*
- 14 SOIL-PILE FOUNDATION INTERACTION, 349**  
Joseph Penzien
- 14.1 Introduction, 349. 14.2 Methods of analysis, 350. 14.3 Determination of soil properties, 360. 14.4 Comments on proposed method of analysis, 368. 14.5 Bridge structural systems investigated, 369. 14.6 Discussion of results, 370. 14.7 Conclusions and recommendations, 380.*
- 15 EARTH SLOPE STABILITY DURING EARTHQUAKES, 383**  
H. Bolton Seed
- 15.1 Introduction, 383. 15.2 Past practice in the evaluation of slope stability during earthquakes, 384. 15.3 Selection of seismic coefficient in pseudostatic analysis, 385. 15.4 New developments in analysis of slope stability during earthquakes, 388. 15.5 Conclusions, 399.*
- 16 CURRENT TRENDS IN THE SEISMIC ANALYSIS AND DESIGN OF HIGH-RISE STRUCTURES, 403**  
Nathan M. Newmark
- 16.1 Introduction, 403. 16.2 Response of simple structures to earthquake motions, 404. 16.3 Response spectra for inelastic systems, 408. 16.4 Multidegree-of-freedom systems, 411. 16.5 Results of elastic analyses for tall buildings, 414. 16.6 Design of composite 41-story building, 419. 16.7 Special considerations, 421. 16.8 Concluding remarks, 423.*
- 17 DESIGN OF EARTHQUAKE-RESISTANT STRUCTURES—STEEL FRAME STRUCTURES, 425**  
Henry J. Degenkolb
- 17.1 Introduction, 425. 17.2 Beam-column connections, 426. 17.3 Bending of beams and girders, 435. 17.4 Columns, 438. 17.5 Repetitive loadings, 441. 17.6 Analysis, 442. 17.7 Diaphragms, 445. 17.8 Summary, 446.*
- 18 DESIGN OF EARTHQUAKE-RESISTANT POURED-IN-PLACE CONCRETE STRUCTURES, 449**  
John A. Blume
- 18.1 Introduction, 449. 18.2 Basic concepts, 450. 18.3 The earthquake performance of poured-in-place reinforced concrete structures, 451. 18.4 Force-deformation characteristics, 452. 18.5 Design requirements and operations, 459. 18.6 Ductile concrete, 465. 18.7 Appendix, 470.*



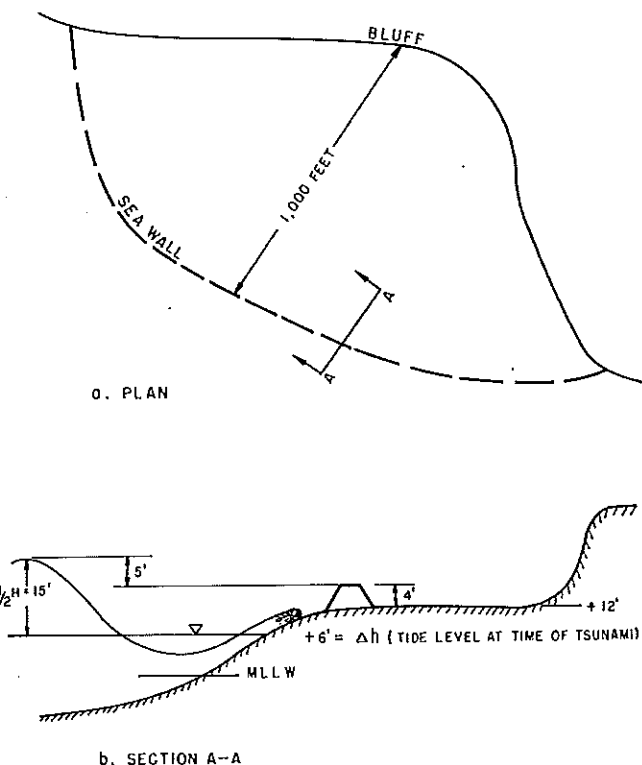


Fig. 11.43. Hypothetical case. (From Wiegel, 1965.)

The action of the March 27–28, 1964, tsunami at Crescent City, California, is an example of an event somewhat of the type described above. There was a small seawall built within the harbor, and the area landward of it was filled with sand. The elevation of the top of the seawall was from about +8 ft above mean lower low water in the most protected region to +13 ft in the least protected region. The fill landward of this wall was from about +10 to +14 ft above mean lower low water. The highest two tsunami waves apparently went over the top and flooded the towns as if the wall were not present. It is evident from Fig. 11.42 that a seawall, to be effective, must be designed to permit only a few feet of overtopping for the “improbable” tsunami and for no overtopping for the “design” tsunami. This is especially true in light of some laboratory experiments by Iwasaki (1965) that showed that the height would be increased at a seawall, at least for waves that are relatively short compared with tsunami waves.

### 11.9 TSUNAMI WAVE FORCES

Few studies have been made of the forces exerted by tsunami waves. In the ocean, and in bays, the waves probably can be treated in the manner of the shorter progressive and standing waves such as swell and seiches. Forces exerted by these types of waves will not

be treated here as there are a number of papers on the subject (see, e.g., Wiegel, 1964d). The forces exerted on structures by tsunami waves running onto the land present a much more difficult problem. No actual measurements of these forces have been made, and only a few estimates of the forces are available.

Matlock, Reese, and Matlock (1962) made a study of the damage to structures in Hilo, Hawaii, caused by the May 23, 1960, Chilean tsunami. They treated the problem as if a bore moved over a dry bed in a manner similar to a surge running downstream from a dam that had failed. They used the equation given by Keulegan (1949) for the approximate speed  $V_s$  of such a surge for the case in which bottom friction is of major importance:

$$V_s = 2\sqrt{gd_s} \quad (11.70)$$

where  $g$  is the acceleration of gravity and  $d_s$  is the height of the surge. A further assumption was made that the water particles, from top to bottom, all moved with the speed of the surge. They examined the numerous observations made of the maximum elevation reached by the highest wave over the land submerged by the highest wave and decided that the crest was at about 15 ft above mean lower low water datum. Finally, they took the vertical distance from the ground to the plus 15-ft level for each particular point of interest in the region from the line of maximum inland inundation ( $d_s = 0$ ) to the line of maximum withdrawal (–7 ft below mean lower low water,  $d_s = 7 + 15 = 22$  ft) and used this as  $d_s$  in Eq. 11.70 to calculate the maximum velocity at that point. Thus, the speed of the bore, and the water within the bore, was assumed to move at speeds between 0 and 53 ft/sec. The observations made by Eaton, Richter, and Ault (1961) indicated that the bore traveled from the breakwater to shore, a distance of about 7000 ft, in from 2½ to 3 min, at a speed of from 40 to 45 ft/sec. This would fix the upper limit of the surge speed, which is not too different from the estimate made by Matlock, Reese, and Matlock. It must be cautioned, however, that practically nothing is known of the velocity distribution within a tsunami as it moves over land.

Matlock, Reese, and Matlock examined in detail 14 cases of structural failure, or near failure, for which they were reasonably certain that secondary causes, such as a drifting log or automobile hitting the structure, were not involved. In all cases but one, they neglected hydrostatic forces and assumed that the horizontal fluid force intensity (pressure) exerted by the flowing waters on the structure was given by the equation

$$p = \frac{1}{2} C_D \rho V_s^2 \quad (11.71)$$

The values of  $C_D$  used in their calculation were the ones normally used in steady flow problems in which the object was completely submerged in a fluid. For one case, a reinforced concrete wall of a building, they



included the hydrostatic force. Their approach was to calculate the forces necessary to cause structural failure and then to use Eq. 11.72 to calculate the velocity necessary to obtain this force. They then compared this velocity with the velocities calculated from Eq. 11.70 and found reasonable correlation.

A theoretical and laboratory study was made by Fukui, Nakamura, Shiraishi, and Sasaki (1963), and they found that the tip of a bore advancing over a dry bed, or in a channel with an initial water depth  $\bar{d}$ , traveled at a speed of

$$V_s = \left( \frac{q\bar{D}(\bar{D} + \bar{d})}{2(\bar{D} - \eta H)} \right)^{1/2} \quad (11.72)$$

where  $\bar{D}$  is the total depth of water in the bore,  $H$  is the bore height ( $\bar{D} - \bar{d}$ ), and  $\eta$  is a resistance term. It was found experimentally that  $\eta$  was equal to about 0.85 (equivalent to a Manning's  $n$  of 0.13) for a dry bed and increased with increasing  $\bar{d}/\bar{D}$  to a value of about 1.03 at  $\bar{d}/\bar{D} = 0.5$  and then remained constant for greater values of  $\bar{d}/\bar{D}$ .

For an initially dry bed,  $\bar{d} = 0$  and  $\bar{D} = H$  (i.e., the equivalent of  $d_s$ ); then Eq. 11.72 becomes

$$V_s \approx 1.8\sqrt{g\bar{D}} = 1.8\sqrt{gH} = 1.8\sqrt{gd_s} \quad (11.73)$$

which agrees rather well with the approximation given by Keulegan (Eq. 11.70). It is interesting to note that all of the bore tip speeds, for the case in which there was an initial depth of water in the channel, were in the region between  $V_s = 2\sqrt{gd_s}$  and  $V_s = \sqrt{gH}$ . They found for the case in which there was an initial water depth in the channel that the bore had a relatively steep front and that the top of the bore was nearly horizontal. It should be pointed out in regard to the "nearly horizontal" top of the bore that the reservoir in the channel was of a fairly limited extent. They found the maximum pressure developed on a vertical wall, which extended the entire width of the laboratory channel, to be

$$p_{\max} = \frac{K_0 \rho g V_s^4}{g^2 d_s} = K_0 V_s^2 \left( \frac{V_s^2}{g d_s} \right) \quad (11.74)$$

This can be expressed as

$$p_{\max} = \frac{1}{2} C_D \rho V_s^2 N_F^2 \quad (11.75)$$

where  $C_D/2 = K_0$  and the Froude number  $N_F$  is given by  $V/\sqrt{gd_s}$ . They found for a vertical wall that  $K_0 \approx 0.5$ , which would be the equivalent of  $C_D \approx 1$ .

It is not clear how Eqs. 11.74 and 11.75 can be used in practice. Three pressure cells were used in one set of tests and six pressure cells were used in another set of tests. The maximum measured pressure was used to determine the exponential of  $V_s$  in Eqs. 11.74 and 11.75, and this maximum might have occurred at a different cell for each bore height.

Dressler (1952, 1954) and Whitham (1955) developed theories for the speed and shape of a surge moving over

a dry bottom in which bottom friction plays a major role. The initial height of water in the reservoir is  $d_0$  above the channel, and  $d$  is the depth of the surge in the channel at some distance  $x$  from the dam at time  $t$ . In the portion of the flow substantially removed from the tip of the surge, the flow can be considered to be the same as for the frictionless case, and the set of parametric equations for  $d$  and the speed  $V$  at this  $x$  and  $t$  can be solved to give the water speed as

$$V = 2\sqrt{gd_0} - 2\sqrt{gd} \quad (11.76)$$

If the flow were frictionless, the speed of the surge tip would be

$$V_s = 2\sqrt{gd_0} \quad (11.77)$$

This, however, is not the case. In fact, the shape and speed of the tip are controlled largely by the friction of the bottom. The results for the tip speed from the theories of Whitham and Dressler are very similar. An average of the results of the two theories is given in Table 11.5. In this table the ratio of the tip speed to  $2\sqrt{gd_0}$  is given as a function of  $Rt\sqrt{g/d_0}$ , where  $R$  is a dimensionless resistance coefficient ( $R = g/C^2$ , in which  $C$  is the Chezy roughness coefficient in the square root of feet per second).

Table 11.5. TIP SPEED FOR SURGE IN A DRY BED

$Rt\sqrt{g/d_0}$	0	0.1	0.2	0.3	0.4	0.5	0.6
$V_s/2\sqrt{gd_0}$	1.0	0.48	0.40	0.35	0.32	0.29	0.26

Cross (1967) made a laboratory and theoretical study of a surge running over a dry bottom (and also over a bottom with a film of water on it) and of the forces exerted by the surge on a structure placed in a channel. He found that the tip speeds were generally a little faster than those shown in Table 11.5, using the appropriate value of the Chezy roughness coefficient. He used both a smooth and a rough bottom in his tests and in his calculations.

In his studies of the shape of the surge tip, Cross found that the theory predicted the shape reasonably well in the immediate region of the tip of the smooth bottom after the surge had run several feet down the channel. However, after the surge had traveled 15 ft or so, the depth of the surge became nearly constant a few feet back from the tip, while the theory showed a continually increasing depth. It should be pointed out that the reservoir used in the experiment was of limited extent, while the theory is for the case of a reservoir of unlimited extent.

Cross also found that when the channel bed had a thin film of water over it (0.015 ft deep) the tip became steeper and the speed of the tip was less, compared with the dry bottom case.

The theory of Cumberbatch (1960) for the force exerted by a fluid wedge impinging on a wall was

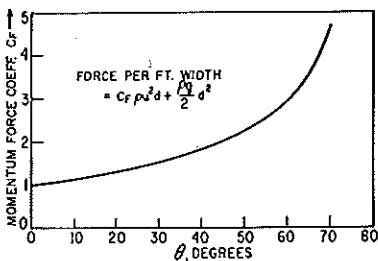


Fig. 11.44. Plot of force coefficient  $C_f$  vs  $\theta$ . (From Cross, 1967.)

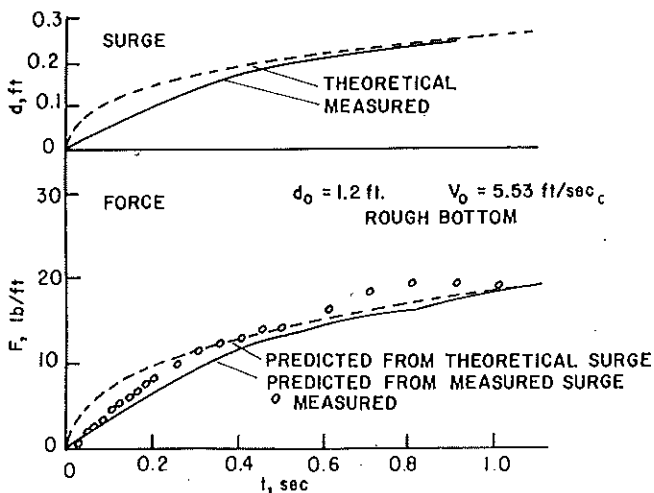
modified by Cross to include the hydrostatic force and was given as

$$F = \frac{1}{2} \rho g d_s^2 + C_f \rho V^2 d_s \tag{11.78}$$

where  $F$  is the force per unit width of wall and  $d_s$  is taken as the height of the surge at the structure, if the structure were not present. Equation 11.78 is for the case of a surge striking a vertical wall extending the entire width of a channel. Cross calculated values of  $C_f$  as a function of the slope of the water surface relative to the horizontal  $\phi$ . The results are shown in Fig. 11.44. The value of  $\phi$  for any time  $t$  at which the surge would be moving past the obstruction were the obstruction not present can be obtained from measurements, or approximately by using the theory of a surge given by Cross.

As an example, one set of measurements is shown in Fig. 11.45, together with the profile calculated from theory using the measured surge tip speed. In this figure  $d_0$  is the original water level in the reservoir prior to the opening of the gate to cause the surge and  $V_0$  is the theoretical velocity of the surge front at the structure were the structure not present. The term "predicted from measured surge" refers to the measurement of a surge that was developed in the channel in a prior test, under identical conditions, but without the vertical wall being installed.

Fig. 11.45. Surge profiles (5/26 data) with predicted and measured force profiles (6/2 data),  $x = 16.33$  ft. (From Cross, 1967.)



Several force records are shown in Fig. 11.46. It can be seen that a force peak occurs at about 0.75 sec after the initial force rise and that then the force remains at about a constant magnitude. The reason for this force peak was studied in detail. The surge, upon striking the vertical wall, ran up the wall a distance approximately equal to  $V_0^2/g$  for the wet bottom case and from  $V_0^2/2g$  to  $V_0^2/g$  for the dry bottom case. This run-up curled back to some extent and then fell, hitting the surface of the reflecting surge. The peak force occurred at the moment this mass of water hit the surface of the reflecting surge.

If the peak force, described above, is neglected, it was found that the "steady" maximum force that occurred (and predicted with a good degree of accuracy by Eq. 11.78 together with Fig. 11.44) is also equal to the hydrostatic force computed using the depth of the reflected surge. Figure 11.44 shows, except near the immediate tip of the surge, that  $\phi$  is small enough for

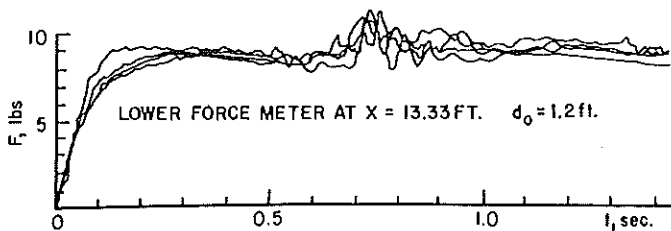


Fig. 11.46. Typical force profiles; smooth bottom. (From Cross, 1967.)

$C_f \approx 1$  to be a valid approximation. Using the further approximation that  $V \approx 2\sqrt{gd_s}$ , and substituting this together with  $C_f \approx 1$  into Eq. 11.78 results in

$$F = 4.5 \rho g d_s^2 \tag{11.79}$$

Now, consider a surge of depth  $d_s$  and velocity  $2\sqrt{gd_s}$ , being reflected by a vertical wall. If no energy is lost, the top streamline will be displaced vertically by  $V^2/2g$  (i.e., by  $2d_s$ ), so that the depth of the reflected surge should be  $d_r = 3d_s$ . Some previous work by the author showed that this was approximately correct, and the studies by Fukui *et al.* (1963) also showed this to be approximately correct for a surge moving in a dry channel. Then,

$$F = \frac{1}{2} \rho g d_r^2 = \frac{1}{2} \rho g (3d_s)^2 = 4.5 \rho g d_s^2 \tag{11.80}$$

which is the same as Eq. 11.77. It must be emphasized that the surge depth  $d_s$  referred to here is taken as the depth of the nearly horizontal portion of the surge a few feet to the rear of the tip.

Cross also made a limited study of the forces exerted by a surge on vertical wall that extended only part way across the channel and found that when the width of the wall was less than about twice the height of the surge, the force started to decrease rather rapidly, with  $C_f \approx \frac{1}{2}$  for a section about one-half the surge height in width.

Laboratory studies similar to Cross's were made by Alavi (1964) for the author, in which the characteristics of surges in a dry bed were studied, together with the forces exerted by the surge on square and circular piles 0.145 ft in diameter. Owing to the restricted width of the channel (0.5 ft) compared with the size of the piles, and owing to the fact that the surge flows are supercritical, the results are only indicative of the forces. The equation

$$F = \frac{1}{2} C_D \rho D d_s V^2 \quad (11.81)$$

was used to express the force, where  $D$  is the pile diameter and  $C_D$  is the coefficient of drag. It was found that  $C_D$  averaged 1.1 for the circular pile and 1.8 for the square pile for Reynolds numbers ( $DV/\nu$ , where  $\nu$  is the kinematic viscosity) between about  $10^4$  and  $10^5$ .

In these studies, Alavi found that there was a linear relationship between  $d_s$  and  $d_o$ , with  $d_s = 0.26d_o$ , at the point where he measured  $d_s$ , about 20 ft downstream from the dam. It was found that  $V_s \approx 2\sqrt{gd_s}$ , for values of  $d_s < 0.2$  ft and  $V_s \approx 2.2\sqrt{gd_s}$ , for  $0.2 < d_s < 0.35$  ft. It was also found that although the maximum run-up on a vertical wall was a function of  $d_s$  (hence,  $V_s$ ),  $d_r/d_s = 3$ .

## REFERENCES

- Abramowitz, M., and I. A. Stegun, eds. (June 1964). *Handbook of Mathematical Functions with Formulas, Graphs, and Mathematical Tables*, National Bureau of Standards, Applied Mathematics Series No. 55.
- Alavi, M. (1964). *Surge Run-up on Sloping Beach, and Surge Forces on Piles*, University of California, Berkeley, College of Engineering, memo to R. L. Wiegel (unpublished).
- Ambraseys, N. N. (October 1962). "Data for the Investigation of the Seismic Sea-Waves in the Eastern Mediterranean," *Bull. Seism. Soc. Am.*, 52 (4), 895-913.
- Amein, M. (1964). *Bore Inception and Propagation by the Nonlinear Wave Theory*, *Proceedings of the Ninth Conference on Coastal Engineering*, ASCE, pp. 70-81.
- Architectural Institute of Japan (December 1961). *General State of Damage of Building, Report on the Chilean Tsunami of Japan, May 24, 1960, as Observed Along the Coast of Japan*, Committee for Field Investigation of the Chilean Tsunami of 1960, pp. 151-164.
- Barber, N. F. (1961). *Experimental Correlograms and Fourier Transforms*, New York: Pergamon Press.
- Bascom, W. (April 16, 1946). *Effect of Seismic Sea Wave on California Coast*, University of California IER, Tech. Rept. 3-204 (unpublished).
- Basset, A. B. (1961). *A Treatise on Hydrodynamics*, 2 vols., New York: Dover Publications.
- Berringhausen, W. H. (October 1962). "Tsunami Reported from the West Coast of South America, 1562-1960," *Bull. Seism. Soc. Am.*, 52 (4), 915-921.
- Borgman, L. E. (August 1963). "Risk Criteria," *J. Waterways and Harbors Div., Proc. Am. Soc. Civil Engr.*, 89 (WW3), 1-36.
- Caldwell, J. M. (1955). *The Design of Wave Channels, Proceedings of the First Conference on Ships and Waves*, Council on Wave Research, The Engineering Foundation, and the Society of Naval Architects and Marine Engineers, pp. 271-287.
- Chen, T. C. (March 1961). *Experimental Study on the Solitary Wave Reflection Along a Straight Sloped Wall at Oblique Angle of Incidence*, U.S. Army Corps of Engineers, Beach Erosion Board, Tech. Memo. No. 124.
- Chester, C., B. Friedman, and F. Ursell (July 1957). "An Extension of the Method of Steepest Descents," *Proc. Cambridge Phil. Soc.*, 53 (3), 599-611.
- Committee for Field Investigation of the Chilean Tsunami of 1960 (December 1961). *Report on the Chilean Tsunami of May 24, 1960, as Observed Along the Coast of Japan*, Tokyo, Japan.
- Cox, D. C. (November 1964). *Tsunami Height-Frequency Relationship at Hilo*, University of Hawaii, Hawaii Institute of Geophysics.
- Cross, R. H. (November 1967). "Tsunami Surge Forces on Coastal Structures," *J. Waterways and Harbors Div., Proc. ASCE*, 93 (WW4), 201-231.
- Cueller, M. P. (February 1953). *Annotated Bibliography on Tsunamis*, U.S. Army Corps of Engineers, Beach Erosion Board, Tech. Memo No. 30.
- Cumberbatch, E. (March 1960). "The Impact of a Water Wedge on a Wall," *J. Fluid Mech.*, 7 (3), 353-373.
- Davison, C. (1936). *Great Earthquakes*, London: T. Murby and Co.
- De Roos, R. and T. Spiegel (September 1966). "The Philippines, Freedom's Pacific Frontier," *Natl. Geograph.*, 130 (3), 301-351.
- Dressler, R. F. (September 1952). "Hydraulic Resistance Effects Upon the Dam-Break Functions," *J. Res. Natl. Bur. Stds.*, 49 (3), 217-225.
- Dressler, R. F. (1954). "Comparisons of Theories and Experiments for the Hydraulic Dam-Break Wave," *IUGG, Rome*, 3, 319-327.
- Eaton, J. P., D. H. Richter, and W. U. Ault (April 1961). "The Tsunami of May 23, 1960, on the Island of Hawaii," *Bull. Seism. Soc. Am.*, 51 (2), 135-157.
- Eckart, C. (April 1948). "The Approximate Solution of One-Dimensional Wave-Equations," *Rev. Mod. Phys.*, 20 (1), 399-417.
- Fraser, G. D., J. P. Eaton, and C. K. Wentworth (January 1959). "The Tsunami of March 9, 1957, on the Island of Hawaii," *Bull. Seism. Soc. Am.*, 49 (1), 79-90.
- Fukui, Y. M. Nakamura, H. Shiraishi, and Y. Sasaki (1963). "Hydraulic Study on Tsunami," *Coastal Engr. Japan*, 6, 67-82.

CONFIDENTIAL BUSINESS INFORMATION

# APPLIED FLUID DYNAMICS HANDBOOK

ROBERT D. BLEVINS

US EPA ARCHIVE DOCUMENT



VAN NOSTRAND REINHOLD COMPANY

CONFIDENTIAL BUSINESS INFORMATION

US EPA ARCHIVE DOCUMENT

Copyright © 1984 by Van Nostrand Reinhold Company Inc.

Library of Congress Catalog Card Number: 83-14517  
ISBN: 0-442-21296-8

All rights reserved. No part of this work covered by the copyright hereon may be reproduced or used in any form or by any means—graphic, electronic, or mechanical, including photocopying, recording, taping, or information storage and retrieval systems—without permission of the publisher.

Manufactured in the United States of America

Published by Van Nostrand Reinhold Company Inc.  
135 West 50th Street  
New York, New York 10020

Van Nostrand Reinhold Company Limited  
Molly Millars Lane  
Wokingham, Berkshire RG11 2PY, England

Van Nostrand Reinhold  
480 Latrobe Street  
Melbourne, Victoria 3000, Australia

Macmillan of Canada  
Division of Gage Publishing Limited  
164 Commander Boulevard  
Agincourt, Ontario M1S 3C7, Canada

15 14 13 12 11 10 9 8 7 6 5 4 3 2

Library of Congress Cataloging in Publication Data

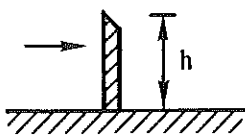
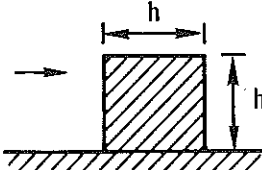
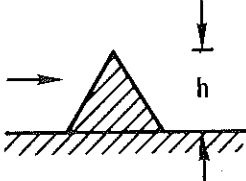
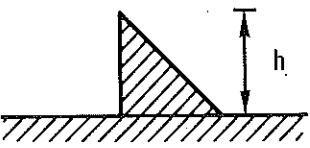
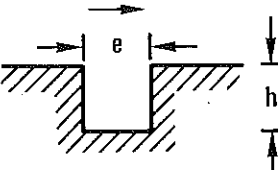
Blevins, Robert D.  
Applied fluid dynamics handbook.

Includes bibliographical references and index.  
I. Fluid dynamics—Handbooks, manuals, etc. I. Title.  
TA357.B57 1984 620.1'064 83-14517  
ISBN 0-442-21296-8



**Table 10-15. Drag of Protuberances.**

Notation:  $C_D$  = coefficient of drag of a protuberance for boundary layer thickness much less than height,  $h \gg \delta$ , where  $\delta$  is the boundary layer thickness and  $h$  is the protuberance height. The drag force is  $F_D = \frac{1}{2} \rho U^2 A C_D$  for  $h \gg \delta$ .  $A$  is the projected area  $A = bh$  for two-dimensional sections and rectangular bodies where  $b$  is width. See text for drag force for  $h$  comparable to  $\delta$ . (Refs. 10-99, 10-102, 10-106, 10-107.) Errors in  $C_D$  of  $\pm 20\%$  can be expected. Also see Tables 10-17 and 10-19 and Chapter 11.

Protuberance	Drag Coefficient, $C_D$ and Remarks
<p>1. Fence Section</p> 	<p>1.4 (also see Fig. 10-14)</p>
<p>2. Square Section</p> 	<p>1.2</p>
<p>3. Equilateral Triangle Section</p> 	<p>1.0</p>
<p>4. Right Triangle</p> 	<p>→ 1.3 ← 1.0</p>
<p>5. Gap Section</p> 	<p><math>0.01 h &gt; e &gt; 0.1 h</math>  <math>0.25 8h &gt; e &gt; 20 h</math>                      (also see Ref. 10-105)</p>

US EPA ARCHIVE DOCUMENT

**Attachment B**  
**Hydraulic Analysis of Lower Ash Pond to**  
**Release of Water from**  
**Economizer Ash Pond**  
**Burlington Generating Station**



SHEET NO. 1 OF 3

PROJECT NO. 154,002,009

DATE 4-1-11

BY TJH CKD MWL

HYDRAULIC ANALYSIS - ECONOMIZER ASH POND  
DISCHARGE FROM LIQ. MASS FLOW

PROBLEM DEFINITION

1.) A SLOPE FAILURE OCCURS IN THE NORTH FACE OF THE ECONOMIZER ASH POND IN THE AREA INDICATED ON FIGURE 1

2.) SHEAR STRESS FROM THE SLOPE FAILURE LIQUIDATES A SUBSTANTIAL VOLUME OF THE ECONOMIZER ASH, FIGURE 2,

3.) THE LIQUIDATED ASH FALLS THE EASTERN HALF OF THE UPPER ASH POND FORCING WATER AND FLUID ASH IN THE UPPER ASH POND TO THE WEST AND NORTH OVER THE TOP OF THE UPPER ASH POND EMBANKMENT AND INTO THE LOWER ASH POND.

WHAT IS THE HYDRAULIC RESPONSE IN THE LOWER ASH POND?

• SOUNDINGS IN THE UPPER ASH POND TAKEN IN 2009 SHOW APPROXIMATELY 5 FT. OF WATER

• NORMAL WATER ELEVATION IN UPPER ASH POND 529 FT AND TOP OF EMBANKMENT 531 FT.

FROM FIGURE 1 DISPLACED WATER IN UPPER ASH POND

$$(5') (700') (300') \approx 1,050,000 \text{ ft}^3$$

US EPA ARCHIVE DOCUMENT



CONFIDENTIAL BUSINESS INFORMATION

UPPER ASH POND

2009

CONCRETE  
TURBINE SITE

ASH POND

ECOMIZER  
ASH POND







SHEET NO. 2 OF 3

PROJECT NO. 154,002.009

DATE 4-1-11

BY TJH CKD MWL

HYDRAULIC ANALYSIS - ECONOMIZER ASH POND  
DISCHARGE FROM LIQ. MASS FLOW

- WATER MUST RISE 2' TO OVER TOP EMBANKMENT
- PART OF WATER BACKS UP INTO WEST END OF UPPER ASH POND

$$(2')(900')(250') \approx 500,000 \text{ ft}^3$$

- REMAINING 500,000 ft<sup>3</sup> GOES OVER TOP OF UPPER ASH POND EMBANKMENT AND INTO THE LOWER ASH POND
- ASSUME TIME RATE OF WATER PUSHED TO LOWER ASH POND SAME AS LIQUIDATED MASS ARRIVAL AT EMBANKMENT P<sub>2</sub> ZONE "ECONOMIZER ASH FLOW CALCULATION."

TIME (MIN)	FF	FLOW (MG)	% COMPLETE	DEPTH (ft)
1	5.3	5.9	69	74
2	6.8	6.9	85	86
3	7.2	7.3	90	91
4	7.4		93	
5	7.5		94	
6	7.6		95	
7	7.7		96	

ASSUME COMPLETE @ 10 MINUTES

90% IN FIRST 3 MINUTES  $0.90 (500,000 \text{ ft}^3) = 450,000$   
 10% IN LAST 7 MINUTES  $0.10 (500,000 \text{ ft}^3) = 50,000$



SHEET NO. 3 OF 3

PROJECT NO. 154,002,009

DATE 4-1-11

BY TJH CKD MWL

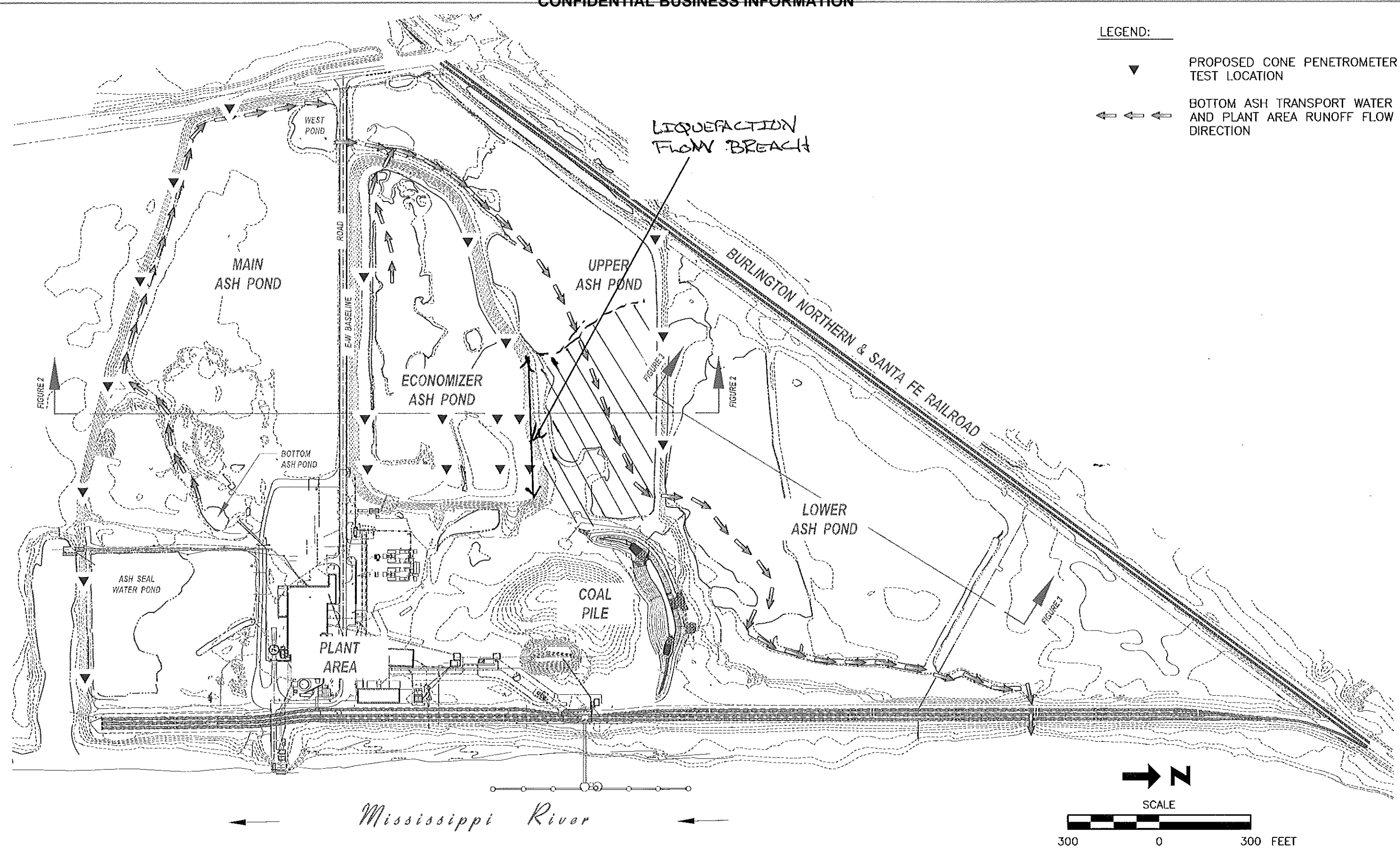
HYDRAULIC ANALYSIS - ECONOMIZER ASH POND  
DISCHARGE FROM LIQ. MASS FLOW

1	
2	
3	BUFFER CAPACITY IN LOWER ASH POND
4	
5	$(1100')(700')(1') = 770,000 \text{ ft}^3 / \text{ft}$
6	
7	TIME 0-3 MINUTES $450,000 \text{ ft}^3 / 770,000 \text{ ft}^3 / \text{ft} = 0.58 \text{ ft}$
8	
9	
10	TIME 3-10 MINUTES $50,000 \text{ ft}^3 / 770,000 \text{ ft}^3 / \text{ft} = 0.065 \text{ ft}$
11	
12	
13	TOTAL RISE IN LOWER ASH POND = $0.58 \text{ ft} + 0.065 \text{ ft}$
14	= 8 INCHES
15	
16	• BEAM AT NORTH END OF LOWER ASH POND
17	IS APPROXIMATELY THREE FEET ABOVE NORMAL
18	FLOW LEVEL
19	
20	• EIGHT INCH WATER SURGE WILL DISCHARGE
21	THROUGH EXISTING OVERFLOW WORK AT INCREASED
22	FLOW RATE
23	
24	• SOLIDS IN WATER SURGE WILL SETTLE IN LOWER ASH
25	POND
26	
27	
28	
29	
30	
31	
32	
33	
34	
35	
36	



LEGEND:

- ▼ PROPOSED CONE PENETROMETER TEST LOCATION
- ←←← BOTTOM ASH TRANSPORT WATER AND PLANT AREA RUNOFF FLOW DIRECTION



US EPA ARCHIVE DOCUMENT

NOTICE  
THIS DRAWING IS THE PROPERTY  
OF AETHER DBS AND IS NOT TO  
BE REPRODUCED, CHANGED, OR  
COPIED IN ANY FORM OR MANNER  
WITHOUT PRIOR WRITTEN  
PERMISSION. ALL RIGHTS RESERVED.

REV	DATE	BY	DESCRIPTION

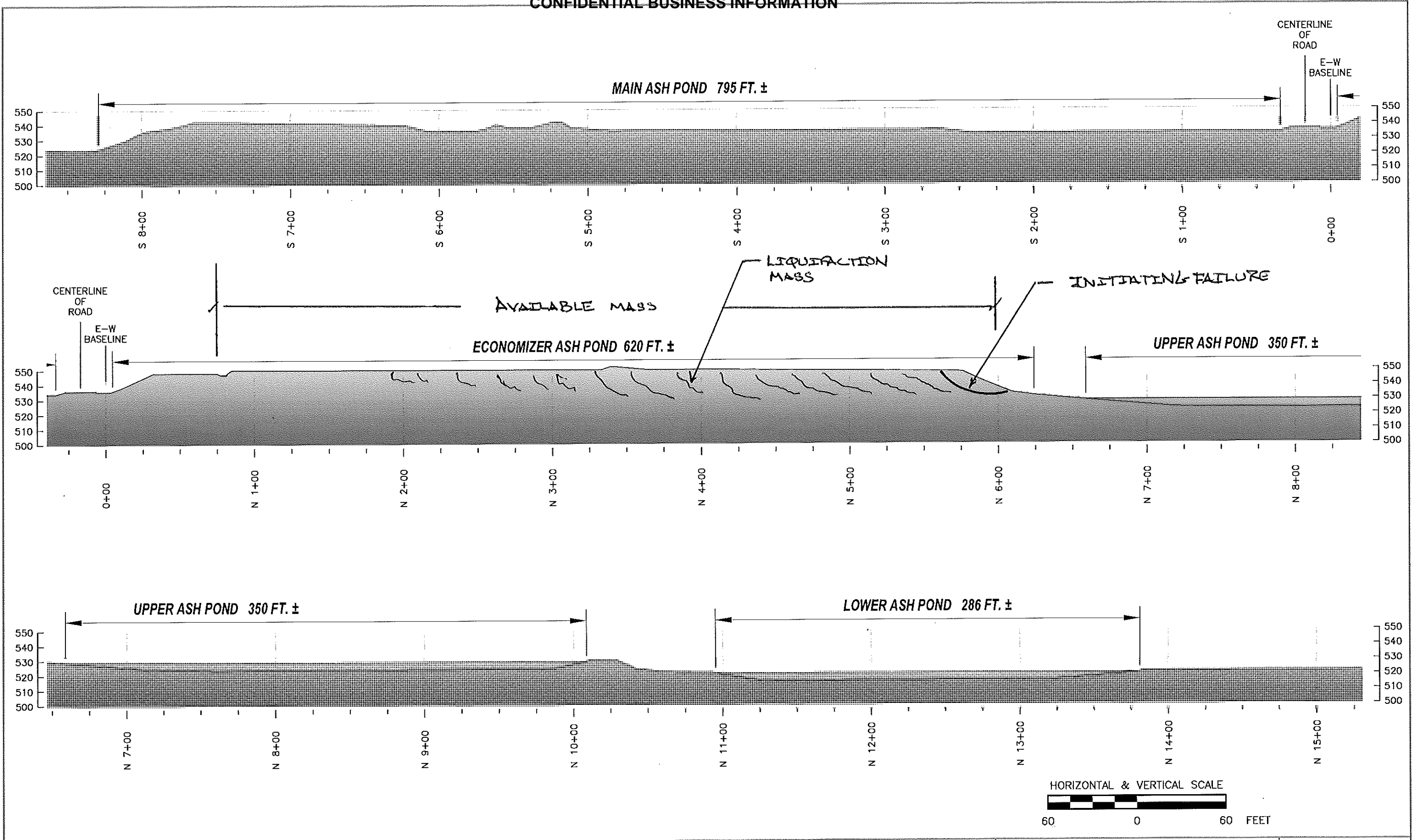



SCALE: AS SHOWN  
DATE: 03-22-11  
DRAWN BY: MM  
CHKD. BY: TCW  
APPROVED: 01-21-11

CLIENT / LOCATION  
ALLIANT ENERGY  
BURLINGTON GENERATING STATION  
BURLINGTON, IOWA

DRAWING DESCRIPTION  
SITE PLAN

JOB 154.002.009  
SHT. 1  
DWG. FIGURE 1

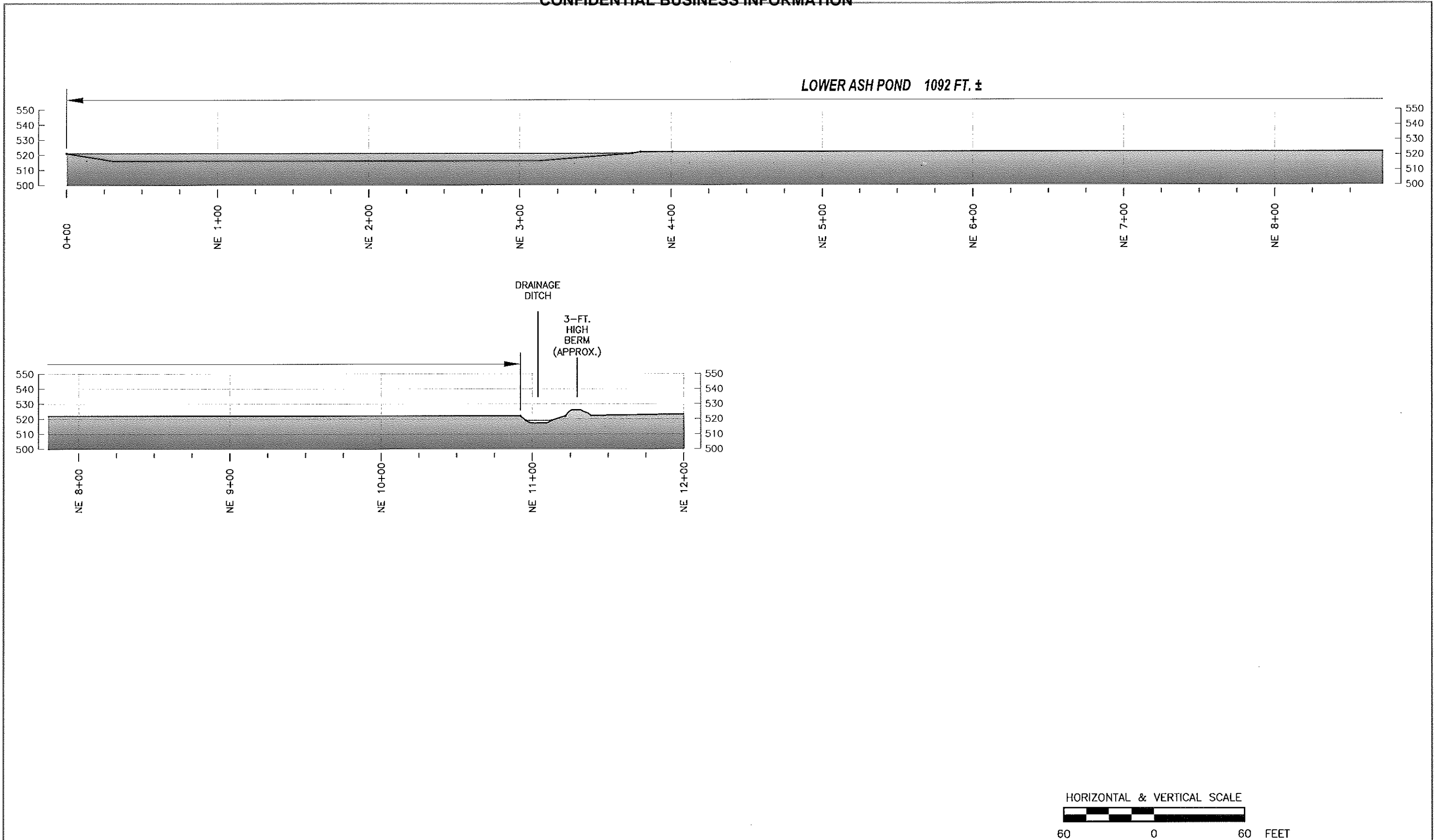


NOTICE THIS DRAWING IS THE PROPERTY OF AETHER DBS AND IS NOT TO BE REPRODUCED, CHANGED, OR COPIED IN ANY FORM OR MANNER WITHOUT PRIOR WRITTEN PERMISSION. ALL RIGHTS RESERVED.	△ △ △ △ △				 www.aetherdbs.com	SCALE: AS SHOWN DATE: 03-22-11 DRAWN BY: MM CHKD. BY: APPROVED:	CLIENT / LOCATION ALLIANT ENERGY BURLINGTON GENERATING STATION BURLINGTON, IOWA	DRAWING DESCRIPTION NORTH - SOUTH CROSS SECTION (VIEW LOOKING WEST)	JOB 154.002.009 SHT. 2 DWG. FIGURE 2
	REV	DATE	BY	DESCRIPTION					

US EPA ARCHIVE DOCUMENT



CONFIDENTIAL BUSINESS INFORMATION

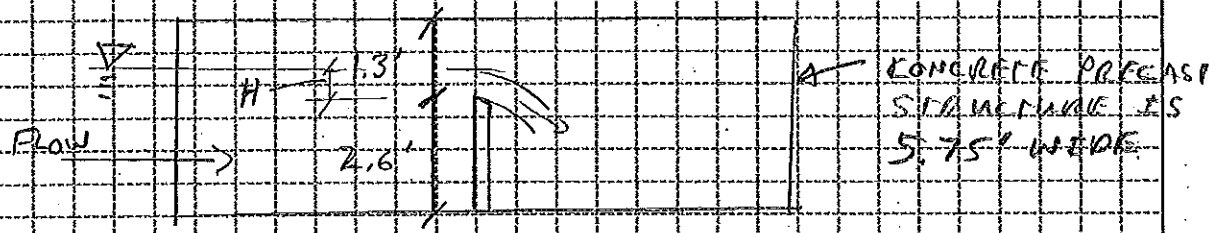


NOTICE THIS DRAWING IS THE PROPERTY OF AETHER DBS AND IS NOT TO BE REPRODUCED, CHANGED, OR COPIED IN ANY FORM OR MANNER WITHOUT PRIOR WRITTEN PERMISSION. ALL RIGHTS RESERVED.				 aether dbS www.aetherdbs.com	SCALE: AS SHOWN DATE: 03-22-11 DRAWN BY: MM CHKD. BY: APPROVED:	CLIENT / LOCATION ALLIANT ENERGY BURLINGTON GENERATING STATION BURLINGTON, IOWA	DRAWING DESCRIPTION NORTHEAST - SOUTHWEST CROSS SECTION (VIEW LOOKING NORTHWEST)	JOB 154.002.009
					SHT. 3			
					DWG. FIGURE 3			
	REV    DATE    BY    DESCRIPTION							



SHEET NO. 1 OF 1  
PROJECT \_\_\_\_\_  
DATE 7/1/11  
BY MWC CKD TJH

RECTANGULAR WEIR CALC.  
LOWER ASH POND

1	
2	
3	
4	① CONCRETE DISCHARGE WEIR IS A
5	SHARP CRESTED RECTANGULAR WEIR
6	
7	WEIR DIMENSIONS
8	
9	
10	
11	
12	
13	
14	
15	
16	
17	
18	② USE THE FOLLOWING EQUATION
19	
20	
21	$Q = CLH^{3/2}$
22	
23	Q = Flow IN FT <sup>3</sup> /S
24	C = DISCHARGE COEFFICIENT = 3.33
25	L = LENGTH OF WEIR = 5.75'
26	H = HEIGHT OF WATER ABOVE WEIR
27	
28	
29	
30	③ CALC H <sub>N</sub> OF NORMAL FLOW
31	
32	Q <sub>AVG</sub> = 3.216 MGD = 4.98 FT <sup>3</sup> /SEC
33	
34	
35	$4.98 \text{ FT}^3/\text{SEC} = (3.33)(5.75 \text{ FT})(H)^{3/2}$
36	
37	$H_N = 0.407 \text{ FT} = 4.89 \text{ IN}$
38	
39	
40	④ IS THE HEIGHT OF THE WEIR SUFFICIENT
41	TO HOLD AVERAGE FLOW PLUS 500,000 FT <sup>3</sup> OF
42	LIQUIDS?
43	
44	$H_L = 0.845 \text{ FT}$ (SEE HYDRAULIC ANALYSIS -
45	ECONOMIZER ASH POND)
46	

US EPA ARCHIVE DOCUMENT





SHEET NO. 2 of  
 PROJECT \_\_\_\_\_  
 DATE 4/1/11  
 BY M.W.L. CKD TJN

RECTANGULAR WEIR CALC (CONT.)  
LOWER ASH POND

1	
2	
3	
4	$H_T = H_L + H_W = 0.407 \text{ FT} + 0.645 \text{ FT}$
5	$= 1.052 \text{ FT}$
6	
7	STRUCTURE HAS 1.3 FT OF FREEBOARD
8	<u>OK</u>
9	
10	
11	
12	⑤ CALCULATE $Q_0$ AT TIME ZERO USING $H_L$
13	
14	$Q_0 = C L H_T^{3/2}$
15	$= (3.33)(5.75')(1.052 \text{ FT})^{3/2}$
16	
17	$Q_0 = 20.66 \text{ FT}^3/\text{SEC}$
18	
19	
20	
21	
22	→ SEE ATTACHED SPREADSHEET FOR
23	FLOW OVER TIME
24	
25	
26	CONCLUSIONS:
27	
28	• WATER FLOW FROM ECONOMIZED LIQUOR ACTION
29	IS THREE TIMES THE AVERAGE FLOW
30	
31	• THE FIRST 25% OF THE DISPLACED
32	WATER WILL DRAIN IN 2.5 HOURS
33	
34	• 50% OF THE DISPLACED WATER WILL
35	DRAIN IN 6 HOURS
36	
37	• 90% OF THE DISPLACED WATER WILL
38	DRAIN IN 24 HOURS
39	
40	
41	
42	
43	
44	
45	
46	

US EPA ARCHIVE DOCUMENT

CONFIDENTIAL BUSINESS INFORMATION

GIVEN:

$C = 3.33$

$L \text{ (ft)} = 5.75$

Area of Lower Ash Pond (sf) = 770,000

$H_T = H_N + H_L = 1.052$

Time (hr)	Time (Day)	Height <sub>T</sub> (ft)	$Q_T \text{ (ft}^3\text{/sec)} = C * L * H^{(3/2)}$	$Q_{AVG} \text{ (ft}^3\text{/sec)}$	$Q_{\text{from liqu}} \text{ (ft}^3\text{/sec)}$	$V_{\text{from liqu}} \text{ (ft}^3\text{)}$	Delta H (ft) = V/A	% of Total	Cumulative	
0.0	0.00	1.052								
0.5	0.02	1.015	20.66	4.98	15.68	28,224	0.03666	5.6%	5.6%	
1.0	0.04	0.981	19.59	4.98	14.61	26,298	0.03415	5.3%	10.9%	
1.5	0.06	0.949	18.61	4.98	13.63	24,534	0.03186	4.9%	15.8%	
2.0	0.08	0.920	17.71	4.98	12.73	22,915	0.02976	4.6%	20.4%	
2.5	0.10	0.892	16.88	4.98	11.90	21,428	0.02783	4.3%	24.7%	
3.0	0.13	0.866	16.12	4.98	11.14	20,059	0.02605	4.0%	28.7%	
3.5	0.15	0.841	15.42	4.98	10.44	18,797	0.02441	3.8%	32.5%	
4.0	0.17	0.818	14.77	4.98	9.79	17,631	0.02290	3.5%	36.0%	
5.0	0.21	0.775	14.18	4.98	9.20	33,105	0.04299	6.6%	42.6%	
6.0	0.25	0.738	13.07	4.98	8.09	29,137	0.03784	5.8%	48.4%	
7.0	0.29	0.704	12.13	4.98	7.15	25,734	0.03342	5.1%	53.6%	
8.0	0.33	0.675	11.31	4.98	6.33	22,800	0.02961	4.6%	58.1%	
9.0	0.38	0.648	10.61	4.98	5.63	20,258	0.02631	4.1%	62.2%	
10.0	0.42	0.625	9.99	4.98	5.01	18,046	0.02344	3.6%	65.8%	
11.0	0.46	0.604	9.46	4.98	4.48	16,113	0.02093	3.2%	69.0%	
12.0	0.50	0.585	8.98	4.98	4.00	14,417	0.01872	2.9%	71.9%	
13.0	0.54	0.568	8.57	4.98	3.59	12,924	0.01678	2.6%	74.5%	
14.0	0.58	0.553	8.20	4.98	3.22	11,606	0.01507	2.3%	76.8%	
15.0	0.63	0.540	7.88	4.98	2.90	10,439	0.01356	2.1%	78.9%	
16.0	0.67	0.527	7.59	4.98	2.61	9,403	0.01221	1.9%	80.8%	
17.0	0.71	0.516	7.34	4.98	2.36	8,481	0.01101	1.7%	82.5%	
18.0	0.75	0.507	7.11	4.98	2.13	7,658	0.00995	1.5%	84.0%	
19.0	0.79	0.498	6.90	4.98	1.92	6,922	0.00899	1.4%	85.4%	
20.0	0.83	0.489	6.72	4.98	1.74	6,264	0.00813	1.3%	86.6%	
21.0	0.88	0.482	6.56	4.98	1.58	5,673	0.00737	1.1%	87.8%	
22.0	0.92	0.475	6.41	4.98	1.43	5,142	0.00668	1.0%	88.8%	
23.0	0.96	0.469	6.28	4.98	1.30	4,664	0.00606	0.9%	89.7%	
24.0	1.00	0.464	6.16	4.98	1.18	4,234	0.00550	0.8%	90.6%	
					<b>TOTAL Discharge</b>	<b>452,904.5</b>			<b>90.6%</b>	

US EPA ARCHIVE DOCUMENT